Open Research Online

The Open University's repository of research publications
and other research outputs

Alteration mineralogy of the Home Plate and Columbia Hills – formation conditions in context to impact, volcanism, and fluvial activity

Journal Item

For guidance on citations see FAQs.

Version: Version of Record

Link(s) to article on publisher's website:
http://dx.doi.org/doi:10.1111/maps.12207

oro.open.ac.uk

Alteration mineralogy of Home Plate and Columbia Hills—Formation conditions in context to impact, volcanism, and fluvial activity

Justin FILIBERTO[1]* and Susanne P. SCHWENZER[2,3]

[1]Department of Geology, Southern Illinois University Carbondale, 1259 Lincoln Road, Mailcode 4324, Carbondale, Illinois 62901, USA
[2]Department of Physical Science, The Open University, Walton Hall, Milton Keynes MK7 6AA, UK
[3]Lunar and Planetary Institute, USRA, 3600 Bay Area Blvd, Houston, Texas, USA
*Corresponding author. E-mail: filiberto@siu.edu

Abstract–The Mars Exploration Rover Spirit investigated the igneous and alteration mineralogy and chemistry of Home Plate and its surrounding deposits. Here, we focus on using thermochemical modeling to understand the secondary alteration mineralogy at the Home Plate outcrop and surrounding Columbia Hills region in Gusev crater. At high temperatures (300 °C), magnetite occurs at very high W/R ratios, but the alteration assemblage is dominated by chlorite and serpentine over most of the W/R range. Quartz, epidote, and typical high-T phases such as feldspar, pyroxene, and garnet occur at low W/R. At epithermal temperatures (150 °C), hematite occurs at very high W/R. A range of phyllosilicates, including kaolinite, nontronite, chlorite, and serpentine are precipitated at specific W/R. Amphibole, with garnet, feldspar, and pyroxene occur at low W/R. If the CO_2 content of the system is high, the assemblage is dominated by carbonate with increasing amounts of an SiO_2-phase, kaolinite, carpholite, and chlorite with lower W/R. At temperatures of hydrous weathering (13 °C), the oxide phase is goethite, silicates are chlorite, nontronite, and talc, plus an SiO_2-phase. In the presence of CO_2, the mineral assemblage at high W/R remains the same, and only at low W/R, i.e., with increasing salinity, carbonate precipitates. The geochemical gradients observed at Home Plate are attributed to short-lived, initially high (300 °C) temperature, but fast cooling events, which are in agreement with our models and our interpretation of a multistage alteration scenario of Home Plate and Gusev in general. Alteration at various temperatures and during different geological processes within Gusev crater has two effects, both of which increase the habitability of the local environment: precipitation of hydrous sheet silicates, and formation of a brine, which might contain elements essential for life in diluted, easily accessible form.

INTRODUCTION

Until recently, the achondrite meteorites shergottites–nahklites–chassignites (SNC) and the orthopyroxenite Allan Hills (ALH) 84001 represented the main source of information about Martian chemistry and mineralogy (e.g., McSween and Treiman 1998; Treiman et al. 2000; Meyer 2010). This changed with the wealth of mineralogy and chemistry data of the surface of Mars revealed by lander and orbiter missions (e.g., Viking landers, Mars Exploration Rovers [MER] Spirit and Opportunity, Phoenix, Mars Pathfinder,

Mars Science Laboratory; and orbiters: Mars Global Surveyor, Mars Odyssey, Mars Express, and Mars Reconnaissance Orbiter). Data from these missions have shown how much diversity in igneous and alteration chemistry and mineralogy there is on Mars that is not seen in the SNC meteorites (e.g., Bibring et al. 2006; Mustard et al. 2008; McSween et al. 2009). For example, the MER Opportunity, which landed in Meridiani Planum, has analyzed abundant secondary minerals not present in the SNC meteorites, from the first outcrop rich in hematite spherules through phyllosilicates at its current location at Endeavour

crater (e.g., Squyres et al. 2004b; McLennan et al. 2005; Arvidson et al. 2011). The MER Spirit, on the other hand, landed in a basaltic region and it was not until it drove to the Columbia Hills, and surrounding deposits, that it experienced extensive alteration mineralogy (e.g., McSween et al. 2006; Morris et al. 2006; Squyres et al. 2006). We use thermochemical models to explore the alteration of a basaltic composition as analyzed by MER Spirit at Home Plate to better understand the diverse alteration mineral assemblages of the Home Plate outcrop and surrounding region of the Columbia Hills.

Home Plate Mineralogy

Home Plate is a plateau in the Columbia Hills of Gusev crater. The structure is roughly 80 m in diameter and approximately 1.5 m thick (Lewis et al. 2008). It is a layered sequence of clastic rocks with alkali basaltic composition, which is interpreted to represent a hydrothermally altered pyroclastic deposit (Squyres et al. 2007; Lewis et al. 2008; Ming et al. 2008; Yingst et al. 2010). The Mars Exploration Rover Spirit has investigated the igneous and alteration mineralogy and chemistry of Home Plate and its surrounding deposits (Squyres et al. 2004a, 2006). Based on thermal emission spectroscopy (TES) and Mössbauer spectroscopy, Home Plate contains igneous olivine, pyroxene, plagioclase, and magnetite with small amounts of hematite and nanophase oxides (Squyres et al. 2007; McSween et al. 2008; Ming et al. 2008; Morris et al. 2008).

Surrounding Home Plate are deposits containing diverse secondary mineral assemblages: Fe^{3+}-sulfate deposits at Paso Robles, Dead Sea, Shredded, Arad, Tyrone, and Troy; hematite-rich outcrops between Home Plate and Tyrone; SiO_2-rich deposits possibly containing pyrite and/or marcasite at Fuzzy Smith; SiO_2-rich, possibly opaline silica, deposits at Northern Valley, Eastern Valley, and Tyrone; montmorillonite at Husband Hill; and Mg-Fe-carbonate outcrops at Comanche in the Columbia Hills (Morris et al. 2006, 2008, 2010; Clark et al. 2007; Wang et al. 2008; Yen et al. 2008; Arvidson et al. 2010; Ruff et al. 2011; Carter and Poulet 2012). These (with the exception of the carbonates) have been interpreted as acid sulfate fumarolic and/or hydrothermal system deposits potentially related to the activity that produced the Home Plate deposit. Bulk chemical data of the Home Plate outcrop support the assumption of high- and low-temperature aqueous alteration because elements more susceptible to alteration show correlations with mineralogy and stratigraphic position within the Home Plate sequence (Schmidt et al. 2008, 2009).

Recent work has suggested that Columbia Hills are possibly the central uplift of an impact crater or the remnants of overlapping crater rims. If indeed Columbia Hills were part of the central uplift of Gusev or overlapping crater rims (McCoy et al. 2008; Parker et al. 2010), the alteration mineralogy seen could be related to impact-generated hydrothermal activity as has been suggested for other locations on Mars from terrestrial analog and modeling work (e.g., Newsom 1980; Allen et al. 1982; Hagerty and Newsom 2003; Abramov and Kring 2005; Schwenzer and Kring 2009b, 2013; Schwenzer et al. 2012a, 2012b) and from orbital observations (Marzo et al. 2010; Mangold et al. 2012). An interesting new observation in Gusev crater is the detection of phyllosilicates (Clark et al. 2007; Carter and Poulet 2012). Although interpreted as sedimentary, some of the phyllosilicates occur in places where the central uplift of Parker et al. (2010) is located.

Here, we build upon previous studies to explore the alteration mineralogy seen at Home Plate using petrologically constrained geochemical inputs and thermochemical models. The results and interpretations of the thermochemical models in this study are applicable to understanding the observed alteration mineralogy and these results will be used to discuss and place constraints on the origin of these deposits. In light of ongoing rover missions, studying the succession and interrelations of events in Gusev and understanding the diversity of alteration assemblages formed by them are critically important. Our results provide insights into MER Opportunity's findings of hydrothermal activity in the rim on Endeavour crater (Squyres et al. 2012), and studying sedimentary processes can provide links to the Mars Science Laboratory Rover Curiosity's landing site, where most recently conglomerates have been found (Williams et al. 2013).

METHODS

We use thermochemical modeling, which is a powerful tool to explore mineral formation, especially where observation is limited (e.g., no isotopic studies are possible). For Mars, a wide range of studies have addressed alteration mineral formation—from carbonates in ALH 84001, to methane production and phyllosilicate formation conditions (e.g., Berger et al. 2009; Bridges and Schwenzer 2012; Chevrier et al. 2007; Griffith and Shock 1995, 1997; Marion et al. 2011; McAdam et al. 2008; Oze and Sharma 2005; Schwenzer and Kring 2009b, 2013; Van Berk and Fu 2012; Wallendahl and Treiman 1999; Zolotov and Mironenko 2007; Zolotov and Shock 1999). While

previous studies have mostly been conducted using Martian meteorite basaltic and dunitic compositions, here we use a starting composition of a basalt that is adjacent, and potentially related, to the alteration mineralogy. Griffith and Shock (1995, 1997) and Schwenzer and Kring (2009a, 2009b) emphasized how important it is to use a starting composition that is relevant to the alteration mineralogy being investigated. Similar work using a starting composition related to alteration products was recently performed for the nahklites (Bridges and Schwenzer 2012). Therefore, our results using a basaltic composition that is temporal to the alteration mineralogy will provide a more robust comparison between the results of our calculations and the actual alteration mineralogy seen in the Home Plate and Columbia Hills region. Furthermore, we use an oxygen fugacity, and chlorine and fluorine concentrations, of the initial basalt composition that are constrained by both the basalts in Gusev crater and Martian meteorites.

We use the code CHILLER (Reed and Spycher 2006) to evaluate mineral assemblages that are likely to form from the Martian Home Plate, Barnhill class rock Fastball in contact with a dilute fluid at various pressures, temperatures, and water to rock ratios (W/R). CHILLER is ideal for this study because it relies on a well-documented and internally consistent thermochemical database of minerals, gases, and aqueous species that allow calculations from ambient temperature to 350 °C, and it has been widely applied to terrestrial basaltic and ultramafic systems (e.g., Reed 1983; Palandri and Reed 2004; Reed and Palandri 2007). Furthermore, we have used CHILLER to investigate alteration Martian mineralogy (Schwenzer and Kring 2009a, 2009b, 2009c, 2013; Bridges and Schwenzer 2012; Schwenzer et al. 2012a). Therefore, these results can be directly compared with our previous results. For input parameters, see also Table 1.

Starting Fluid Composition

The starting fluid determines important parameters in the models, because any species added in high concentration will imprint its effects on the model results (see CO_2 below). To be directly comparable to previous work, we use the same fluid composition (Schwenzer and Kring 2009a, 2009b, 2013; Bridges and Schwenzer 2012; Schwenzer et al. 2012a). The aqueous fluid composition is based on observed terrestrial fluids (approximately 70 °C) venting from basaltic environment (Deccan Traps; Minissale et al. 2000). The composition is adjusted for Martian basaltic compositions by taking the Ca concentration of the terrestrial fluid and adjusting the Mg and Fe using the

Table 1. Input parameters for models: Host rock and starting water compositions.

Fastball oxide	wt%	Starting water species	Mole in 1 kg of H_2O
SiO_2	45.30	Cl^-	5.87E-02
Al_2O_3	7.85	SO_4^{2-}	2.85E-03
FeO	16.92	HCO_3^-	1.68E-05
Fe_2O_3	0.60	Ca^{2+}	2.50E-03
MgO	12.00	Mg^{2+}	2.05E-02
CaO	4.83	Fe^{2+}	9.19E-03
Na_2O	2.35		
K_2O	0.23		
TiO_2	0.67		
MnO	0.47		
P_2O_5	0.79		
CaF_2	1.23		
$CaCl_2$	0.94		

ratios observed in Martian rock. This starting fluid was then used for our calculations, starting the modeling at very high W/R ratios. This causes equilibrium with the modeled rock composition, especially for fO_2 and the least soluble elements such as Al, and Fe. With this procedure, we ensure that we have a dilute brine containing the most important cations, but do not interfere with the model results by adding species to the system. We effectively model a system containing rock + water only, except for the cases with CO_2-addition. CO_2 was set in the fluid to 0.2×10^{-4} mole HCO_3^-, which is the amount of CO_2 in equilibrium with today's Martian atmosphere. No additional source of CO_2 was assumed. To explore the effect of CO_2, we added 0.5 mole HCO_3^- to the solution, following our earlier models on ALHA84001 (Schwenzer and Kring 2009c) and the nahlites (Bridges and Schwenzer 2012).

Starting Basaltic Composition

To calculate the most relevant alteration mineralogy for the Home Plate region of Mars, we have chosen our input parameters based on the petrology and geochemistry of the Home Plate outcrop and where the data from the MER Spirit were lacking, we rely on the geochemistry of Martian meteorites. We chose the Fastball bulk composition as our starting rock composition, because it has the least amount of Cl and SO_3 of all of the Home Plate basalts, suggesting that it is the least altered composition (Squyres et al. 2007). Furthermore, Filiberto et al. (2010) have recently shown that it represents a primitive basaltic composition, while the other basalts analyzed at Home Plate are fractionated basalts (Filiberto and Dasgupta 2011).

Therefore, the bulk composition is more typical of a basalt directly produced from a bulk mantle source region and has not undergone secondary processes. We set the oxygen fugacity of Fastball in our calculations to 2 log units below the QFM oxygen fugacity buffer equivalent to approximately 10% of FeO_T as Fe_2O_3. While we do not know the exact oxygen fugacity of the Home Plate basalts, this value was chosen based on the average values for the SNC meteorites (e.g., Herd et al. 2002; Goodrich et al. 2003; Herd 2003) and is consistent with model oxygen fugacity values for the Home Plate basalts (Schmidt et al. 2011). Because we assume a system of water + rock only, we decided on the oxygen fugacity that is defined by our understanding of the petrology of this rock and transfer this into the model by the partitioning of Fe between FeO and Fe_2O_3 in the input data. Note that the oxygen fugacity of the alteration products is controlled by this choice for the host rock and during the run is a free parameter depending solely on the minerals formed. Finally, 0.3 wt% of F and Cl as CaF_2 and $CaCl_2$ were added to the bulk composition. The analysis of Fastball suggests that it has 1.7 wt% Cl; however, this high Cl content is most likely from hydrothermal alteration and not the original magmatic concentration (Schmidt et al. 2008). Therefore, we have chosen 0.3 wt% Cl. This value is consistent with both the unaltered ("ratted") surface of the Adirondack class basalts and estimates for some SNC meteorites (McSween et al. 2006; Filiberto and Treiman 2009). While F cannot be analyzed by the MER Spirit, we have based this composition on the F/Cl ratio of the SNC meteorites (Dreibus and Wänke 1985; Filiberto and Treiman 2009).

Sources and Concentration of Carbon Species

In principle, five sources for carbon are possible: the Martian atmosphere, ground ice/clathrates, the dissolution of a carbonate precursor, a degassing magma, or carbonaceous chondrite material. If the Martian atmosphere is the source of the CO_2, the dissolved carbon dioxide concentration varies with temperature and the partial pressure of CO_2 in the atmosphere. Henry's law calculations (at 25 °C) for 0.1, 1, and 10 atom result in 0.15, 1.5, and 15 g L^{-1} CO_2 in solution, respectively. In addition to being controlled by atmospheric pressure and composition, the solubility of CO_2 in the fluid is highly dependent on fluid temperature and salinity (e.g., Barnes 1997; Diamond and Akinfiev 2003). Ices and clathrates can contain a highly variable amount of CO_2, because the CO_2 concentration is dependent on the formation temperature of the ice (below approximately −56 °C CO_2 itself forms ice). Potential precursor carbonates

could contain between 0.38 and 0.52 g of CO_2 in one g of carbonate for Mg- and Fe-carbonates, respectively. Degassing from the magma can also provide CO_2 to the system and the CO_2 flux from volcanic eruptions has been potentially linked to an early greenhouse Martian atmosphere (Hirschmann and Withers 2008; Stanley et al. 2011, 2012). CO_2 solubility in a magma decreases with decreasing pressure, thereby exsolving a CO_2 vapor upon eruption and potentially driving an eruption (e.g., Dixon and Stolper 1995; Dixon et al. 1995). Fastball is in equilibrium with the Martian mantle at 1.2 GPa (Filiberto et al. 2010) corresponding to a maximum solubility of approximately 0.5 wt% dissolved CO_2 before eruption and degassing (Stanley et al. 2012). Upon eruption, CO_2 solubility in the Fastball magma would drop to approximately 0 wt% and CO_2 would be released to the surrounding environment and available for alteration. Finally, carbonaceous chondritic material, which makes up 1–3% of the Martian crust, can also contribute carbon to the region and alteration products (Yen et al. 2006). With several CO_2 sources possible, we adopt 22 g CO_2 kg^{-1} of solution, i.e., 0.5 mole per kg of solution as our model CO_2 content. We note that this probably exceeds the amount from atmospheric CO_2 input, but could be achieved from other CO_2 sources.

Further Model Parameters

To explore different stages of the hydrothermal system, we calculated mineral assemblages at three temperatures (13, 150, and 300 °C), P = 110 bar, and water to rock ratios (W/R) from 100,000 to 1. 110 bar equals to about 1 km depth, hence 13 °C is our lowest temperature modeled to account for the Martian geothermal gradient. We chose these conditions to cover a wide range of potential conditions for the formation of alteration assemblages. pH and fO_2 were calculated as a result of the rock and fluid interaction, i.e., controlled by the mineral-forming reactions rather than forcing the model to a certain fO_2. This is justified by the observations in the nakhlites that the system becomes more oxidizing as the precipitation progresses (Changela and Bridges 2010; Hicks et al. 2012).

An important parameter is W/R, which is measured in gram of rock per g of water and can be viewed as a reaction progress variable. To transfer the model W/R to nature, one should bear in mind that W/R in any natural rock can vary on small and large scale. The highest W/R is observed on exposed surfaces facing an open fracture or the atmosphere (if there is precipitation). Intermediate W/R is the result of water flow through highly porous rocks, and low W/R occurs,

where water flow is most restricted. W/R can vary on large, i.e., outcrop, scale and within that variation again on smaller hand specimen and thin section scales. If the influx of unreacted water is limited, then the W/R decreases with time due to more and more of the rock reacting with the brine over time.

MODEL RESULTS

300 °C Subsurface Alteration

Alteration at 300 °C requires the alteration to take place in the subsurface to avoid boiling of the fluid. Much higher temperatures are unlikely to be observed with orbiter or rover capabilities, because terrestrial examples show that they are rarely preserved (e.g., Browne 1978). As carbonates do not form at this high temperature, we will only discuss the CO_2-poor case (Fig. 1), whereby only phases with >5% abundance are shown in the figure. If W/R is high, most ions stay in solution and the precipitates are dominated by Fe (and Al)-oxides. The main precipitate is magnetite, and the trace phase, at very high W/R, is diaspore. At an intermediate W/R of approximately 1000 chlorite, serpentine, and magnetite are the main precipitates, with fluorite, fluor-apatite, and pyrite as minor or trace phases. At a low W/R of approximately 10, chlorite, serpentine, quartz, pyroxene, and epidote are the main phases, with garnet, fluor-apatite, fluorite, and feldspar as minor and trace phases.

150 °C Subsurface Alteration

Similar to models at 300 °C, alteration at 150 °C requires a subsurface position to avoid boiling, but unlike at higher temperatures, carbonates do precipitate in the presence of CO_2 or carbonate dissolved in the fluid. Figure 2 shows both cases, CO_2-poor (panel A) and with 0.5 mole CO_2 (panel B).

In the CO_2-poor case, and at high W/R, hematite is the main phase to precipitate with minor pyrite and diaspore. With CO_2 present, all Fe is precipitated as carbonate, and Al is precipitated as kaolinite—but in very small quantities at very high W/R. At intermediate W/R, in the CO_2-poor case, nontronite, hematite, and kaolinite dominate the assemblage with minor pyrite and ± quartz; in the presence of 0.5 mole CO_2, carbonate, kaolinite, and an SiO_2-phase (likely quartz at high T) are the main minerals, with traces of apatite and ±nontronite. At low W/R, the mineral precipitates resemble a "metamorphic" assemblage with chlorite, amphibole, and quartz being the main minerals; minor constituents are garnet and serpentine; and accessory phases are fluor-apatite,
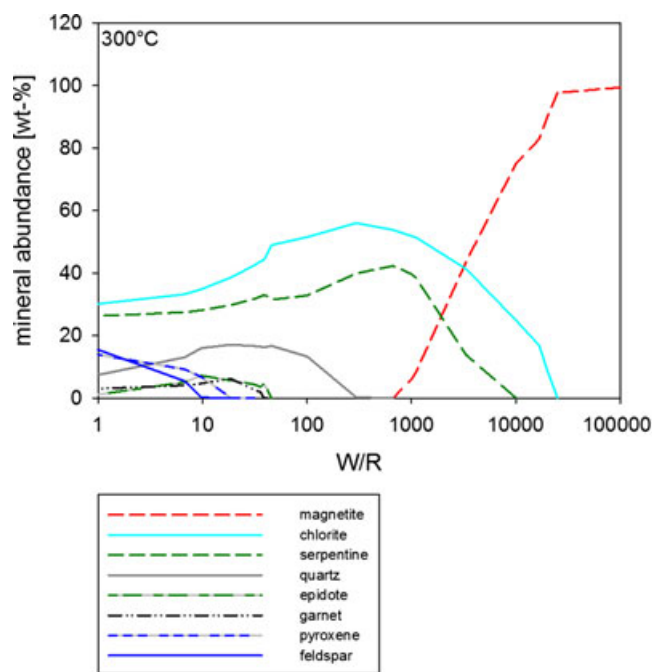

Fig. 1. Model alteration phases at 300 °C. Shown are phases with >5% abundance. Trace phases are diaspore at very high W/R, magnetite, fluor-apatite, and pyrite at intermediate W/R (W/R = 1000), and fluorite, fluor-apatite, and garnet at low W/R (W/R = 10).

fluorite, and pyrite. In the CO_2-containing case, chlorite, carbonate, and quartz are the main phases, with minor/accessory carpholithe, fluor-apatite, nontronite, and fluorite.

13 °C Subsurface Alteration

Alteration at 13 °C is dominated by phyllosilicates even in the dilute case. Nontronite and chlorite are the silicate phases, and goethite is the Fe-oxide. This assemblage is formed at high and intermediate W/R. With decreasing W/R, but still in the intermediate range, a SiO_2-phase and talc occur. At low W/R, amphibole shows up in the model, but is likely not forming for kinetic reasons. Zeolite forms at low W/R, too. With the F-content assumed for the model, fluorite forms at intermediate and low W/R, reaching up to 2% abundance. Other trace minerals are alabandine and mica.

The presence of CO_2 does not change the precipitated mineral assemblage at high to intermediate W/R. Beginning with intermediate W/R and toward low W/R carbonate and SiO_2-phase form. Again, we do not expect the amphibole to form for kinetic reasons. Trace phases not displayed in Fig. 3 are fluorite, apatite, graphite, and talc.
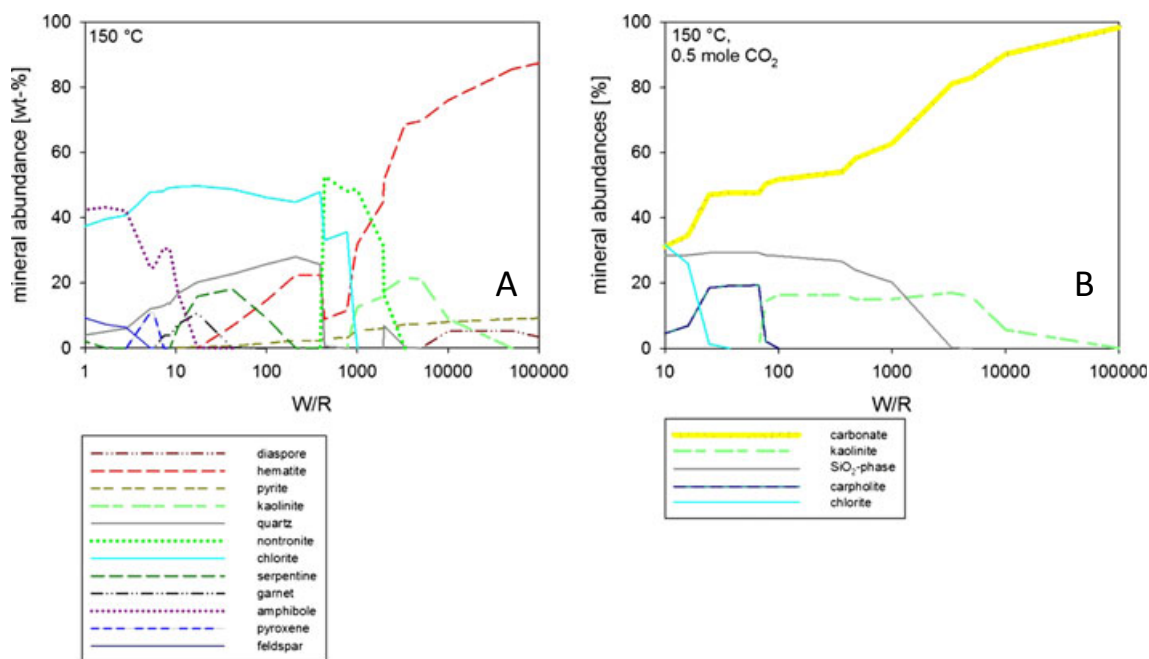
Fig. 2. Alteration at 150 °C with low and with 0.5 mole CO_2. Shown are phases above 5 wt% only. For traces, see text. Panel A: low CO_2 content, panel B: 0.5 mole H_2CO_3.
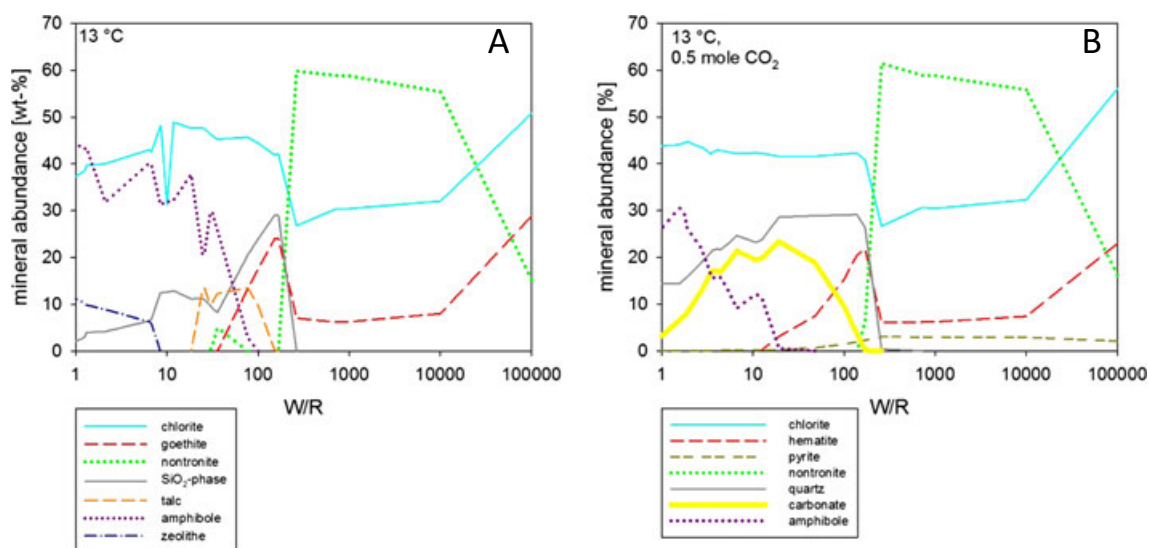

Fig. 3. Alteration at 13 °C with low and with 0.5 mole CO_2. Shown are phases above 5 wt% only. For traces, see text. Panel A: low CO_2 content, panel B: 0.5 mole H_2CO_3.

Fluid Composition Associated with the Minerals

Figure 4 summarizes the different water compositions for fluid-forming minerals at all temperatures and CO_2 concentrations shown in Figs. 1–3, for W/R of 1000 and 10. We chose these W/R, because a W/R of 1000 is in the range of the smectite formation and thus the most likely fluid

forming in association with the observed phyllosilicate minerals and carbonates, which are in close proximity to the silica deposits; and we choose a W/R of 10 because it is a more concentrated fluid, and will precipitate higher amounts and a greater diversity of minerals. For a more detailed insight, we also show the selected elements in the fluid plotted against the SiO_2 content of the fluid (Fig. 5).
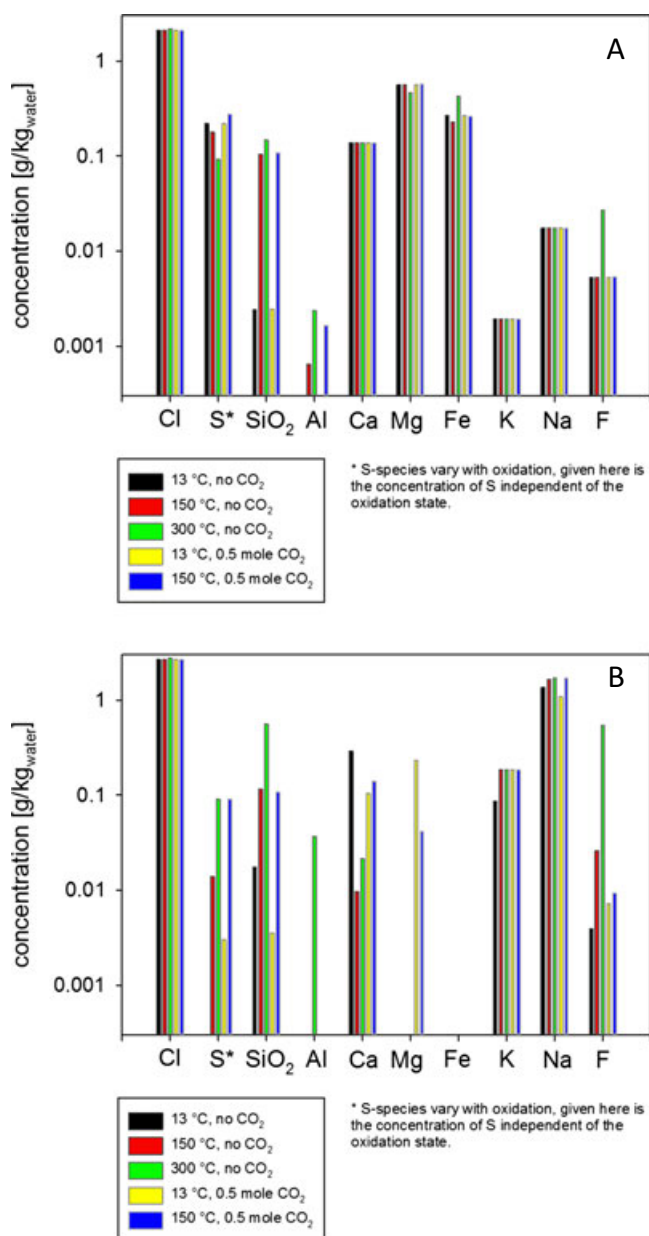
Fig. 4. Fluid composition corresponding to the alteration assemblages at W/R = 1000 (upper panel) and W/R 10 (lower panel) as plotted in Figs. 1–3 and described in the text. Note that no oxidation state is given, i.e., sulfur species and $Fe^{2+/3+}$ ratios are not specified.

At W/R of 1000, pH of these fluids is in the neutral range for the CO_2-poor case, i.e., 6.0, 4.0, 3.4 at 13, 150, and 300 °C, respectively. Fluids with 0.5 mole CO_2 are at pH 6.0 and 3.4 at 13 and 150 °C. Note that the dissociation constant of water is shifted toward lower values with increasing temperature (minimum K_w approximately 250 °C; Bandura and Lvov 2006). CO_2 is dissolved as carbonic acid, for

which reason the dissociation behavior of this species dominates the pH.

Calcium, potassium, and sodium have the same concentrations in the fluid at all temperatures (but are dependent on the amount of rock dissolved), because no phase is formed that precipitates them. Cl and F show higher concentrations in solution at 300 °C only, because apatite precipitation is lacking at W/R 1000 and high temperature, while it precipitates at lower temperatures. Mg is precipitated in chlorite and nontronite, and Fe is precipitated in nontronite, Fe-oxide, or -hydroxide, and pyrite. Carbonate precipitation is only relevant at 150 °C, where it replaces hematite in the CO_2-poor model. At 13 °C, carbonate formation sets in at lower values only due to the increased solubility of CO_2 at lower temperature. Al is the least soluble element under the given conditions and most of it is precipitated as diaspore or kaolinite with only negligible amounts left in solution. Al is most soluble at 300 °C. Note the higher SiO_2-concentration in the fluid with increasing temperature.

At W/R of 10, a factor of 100 more rock is present in the system and the fluid has a higher salinity. Precipitation removes iron from the solution in all five models. Aluminum is precipitated completely except at 300 °C. Mg is precipitated in silicates, but not to the same extent when carbonate precipitation takes place. K and Na stay mostly in solution.

In summary, the fluids produced under any of the alteration conditions carry Na, K, Ca, and Cl and could lead to the formation of chlorides upon evaporation of the brine. For the other elements, concentrations vary with W/R and temperature. Iron is transported by the dilute brine, and could therefore form oxides/hydroxides and/or sulfides/sulfates, depending on redox conditions and other minerals present. Ca provides an alternate sink for S-species, if Ca-sulfates become stable. The amount of fluorine in the solution is controlled by the amount of apatite and amphibole, but also if fluorite becomes stable in the precipitation at the alteration site, which in turn is a sink for Ca. SiO_2 shows two interesting trends: (1) the higher the alteration temperature, the more SiO_2 is carried by the solution, and (2) carbonate-bearing solutions carry slightly more SiO_2.

COMPARISON WITH PREVIOUS MODEL RESULTS

While many studies have used thermochemical modeling to investigate alteration mineralogy produced from diverse bulk compositions, water chemistry, and alteration conditions, we focus our direct comparison on the benchmark papers of Griffith and Shock (1995,
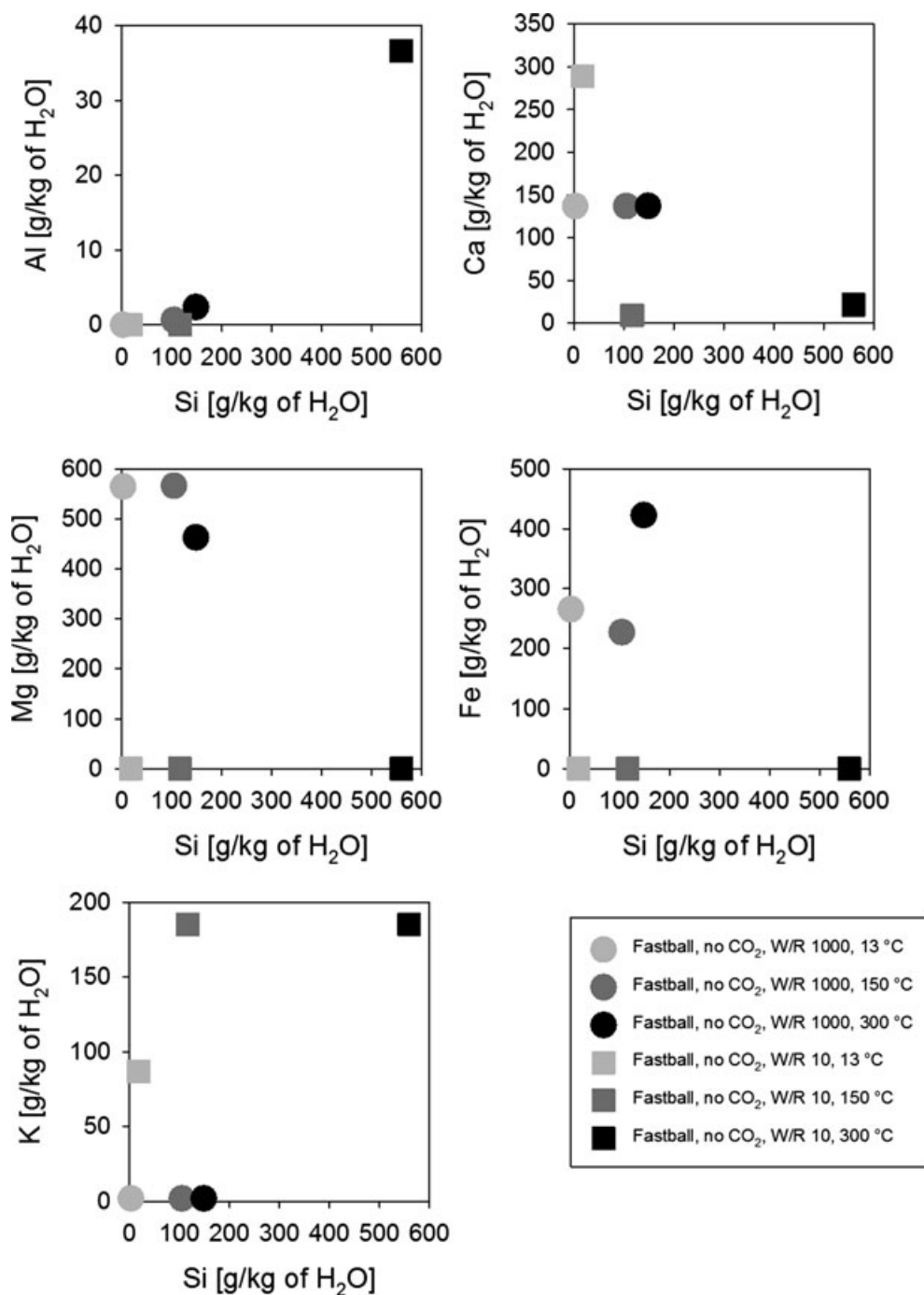
Fig. 5. Fluid composition corresponding to the alteration assemblages from CO_2-poor fluid at W/R = 1000 and 10 as plotted in Figs. 1–3 and described in the text.

1997), and work by Schwenzer using CHILLER on different rock compositions and in various alteration scenarios.

The benchmark papers of Griffith and Shock (1995, 1997) explored the possible storage of water and carbon dioxide in alteration minerals in the Martian crust. Griffith and Shock (1997) investigated how much water can be taken up by alteration mineralogy of different terrestrial magma compositions, the Martian basalt Shergotty, and the Martian dunite Chassigny. They concluded that the host rock composition, along with temperature, is the major control on hydrous mineral production and that altering a rock with the Shergotty bulk composition produces a range of hydrous minerals

that can accommodate up to 8 wt% hydroxyl. Griffith and Shock (1995) investigated the effect of carbon on alteration products of a Shergotty bulk composition. They concluded that chlorite, carbonate, tremolite, albite, and quartz are the calculated alteration assemblage. Furthermore, Wallendahl and Treiman (1999) modeled the alteration of the Martian basalt Shergotty at temperatures <150 °C and calculated two distinct mineral assemblages: (1) for an open-system conditions with CO_2 buffered at 6 mbar: clays, cabonates, quartz, a near neutral pH water, and (2) for a closed system when CO_2 is not externally buffered: clays, serpentine, diopside, H_2-rich and CH_4-rich gas, and alkaline water near pH 12. These assemblages are consistent with both terrestrial and Martian alteration assemblages, but are significantly different from the results of Griffith and Shock (1995, 1997) because the Griffith and Shock work was conducted with a fixed fO_2. Similar to Wallendahl and Treiman (1999), our results are comparable to those from terrestrial systems. At low temperatures, phyllosilicates dominate the assemblage with nontronite and chlorite as the silicate phases, and goethite is the Fe-oxide. For a CO_2-rich system, all Fe is precipitated as carbonate, and Al is precipitated as kaolinite—but in very small quantities at very high W/R. As has been suggested by Griffith and Shock (1995, 1997), our results confirm that there could be an extensive reservoir of carbonate and hydrous minerals produced by alteration of Martian basalts in the Martian crust today.

Focusing on hypervelocity impact as a heat source, resulting hydrothermal alteration mineralogy has been modeled for a variety of host rocks and a wide temperature range (Schwenzer and Kring 2009b, 2013; Bridges and Schwenzer 2012; Schwenzer et al. 2012a). Schwenzer and Kring (2009b) used the code CHILLER (Reed and Spycher 2006; which we use here) to calculate alteration minerals that form from a plutonic shergottite composition (LEW88516). Their calculations produced serpentine-dominated lithologies at low water-to-rock ratios (W/R), nontronite-dominated lithologies at intermediate W/R, and hematite-dominated lithologies at high W/R. Continuing to investigate the effect of impacts on hydrothermal mineralogy, Bridges and Schwenzer (2012) have modeled formation conditions of the secondary minerals produced by alteration of a Lafayette bulk composition to match the observations (Changela and Bridges 2010). Their results showed a comparably high temperature associated with high CO_2-presence for carbonate precipitation, followed by cooling of the fluid toward the smectite precipitation. The last phase observed is a gel of smectitic composition (Changela and Bridges 2010), which is the result of even more rapid cooling. Our results are significantly different from Bridges and Schwenzer (2012) due to the significant differences in bulk chemistry, and are more similar to the work on LEW 88516 (Schwenzer and Kring 2009b). For our models, carbonates do not form at high temperature and only form at temperatures at or below 150 °C. At 150 °C and intermediate W/R, in the CO_2-poor case, nontronite, hematite, and kaolinite dominate the assemblage with minor pyrite and ± quartz; in the presence of 0.5 mole CO_2, carbonate, kaolinite, and an SiO_2-phase (likely quartz at high T) are the main minerals.

HOME PLATE ALTERATION MINERALOGY IN CONTEXT

As outlined in the introduction, Home Plate is surrounded by deposits of diverse secondary mineral assemblages (Morris et al. 2006, 2008, 2010; Wang et al. 2008; Arvidson et al. 2010; Ruff et al. 2011; Carter and Poulet 2012). We will now constrain their formation history.

Hematite

Hematite-rich outcrops have been investigated at Low Ridge between Home Plate and Tyrone (e.g., Arvidson et al. 2008; Morris et al. 2008). Fe-oxides and hydroxides precipitate in all models, as magnetite, hematite, or goethite, depending on temperature. In all cases, they are the dominating or among the most abundant phases at high W/R, but precipitate over wide W/R. Conditions for dominating precipitation from solution are best met at near neutral conditions (because of their amphoteric nature), and when the Si and CO_2 concentrations are below that for silicate resp. carbonate formation. Hematite is a common mineral in our calculations, especially at high W/R ratios and intermediate temperatures (150 °C, Fig. 2). If it is found in spatial relationship with other alteration products or a vein wall, it indicates hydrothermal conditions. At lower temperatures, the direct product would be goethite. However, all Fe-oxide and hydroxide phases can mature into one another depending on subsequent conditions (Cornell and Schwertmann 2003), a fact which has been experimentally investigated for the Meridiani Planum region (Tosca et al. 2008). Therefore, our models confirm very high W/R, if the goethite/hematite is observed in alteration mineralogy context, but cannot account for later maturation.

Sulfates

Fe^{3+}-sulfate deposits have been analyzed at Paso Robles, Dead Sea, Shredded, Arad, Tyrone, and Troy

Table 2. Sulfur species (expressed as gypsum) and SiO_2 in g contained in one kg of solution at all conditions modeled and W/R of 1000 and W/R of 10.

T [°C]	13	Without CO_2		With CO_2	
		150	300	13	150
W/R = 1000					
Gypsum	0.35	0.29	0.42	0.35	0.44
Silica	0.002	0.10	0.15	0.002	0.11
W/R = 10					
Gypsum	0.002	0.07	0.44	0.01	0.44
Silica	0.02	0.12	0.56	0.004	0.11

(e.g., Ming et al. 2006; Morris et al. 2006). Fe-sulfates do not form in our models directly as a result of altering the basalt, because S-species are not concentrated enough in comparison with other species competing for Ca and Mg (e.g., silica); however, cooling of the fluid can precipitate sulfates. At a W/R = 1000, sufficient amounts of both, Fe and S, stay in solution and therefore Fe^{3+}-sulfate would precipitate upon cooling of the fluid (Fig. 4). At a lower W/R (=10). S stays in solution, but Fe reacts out and no Fe^{3+}-sulfates would form; instead, gypsum would form from solution. Furthermore, at W/R of 10 and 13 °C in the presence of CO_2, there is a minimal amount of S-species left in solution. The reason is the more reducing environment in the presence of CO_2, which leads to pyrite precipitation at the site of alteration. Therefore, less S-species are available in solution. The maximum amount of sulfur in solution is equivalent to 0.44 g of gypsum per kg of solution (Table 2). Note, however, that this is the maximum amount of sulfates that could be produced from the amount of sulfur present—and might require additional cations.

Opaline Silica

SiO_2 concentration in the fluid is directly dependent on temperature (Fig. 4): SiO_2 concentrations increase with increasing temperature and decreasing W/R, or—of course—higher water flow rates. At comparable water flow, more silica will be transported, the higher the alteration temperature and the lower the W/R. The occurrence of silica deposits at and around Home Plate supports the assumption of efficient silica transport by hydrothermal solutions. These have been interpreted as acid sulfate fumarolic and/or hydrothermal system deposits potentially related to the activity that produced the Home Plate deposit (Squyres et al. 2008; Rice et al. 2010; Ruff et al. 2011). McAdam et al. (2008) calculate that alteration of an olivine basalt from cold, acidic fluid activity would deposit as much as 500 g per kg of rock at pH below 4 and W/R of 1000. In other words,

0.5 g of amorphous silica is potentially deposited from one kg of solution from acidic fumaroles, but this requires very low pH. In our calculations, we reach a similar amount of precipitation at a pH in equilibrium with the country rock: there is 0.56 g SiO_2 per kg in the CO_2-poor solution at 300 °C. The difference between both models lies in the fact that for cold water precipitation, acidic pH is necessary (or much lower amounts of SiO_2 are dissolved; Table 2). To explore the silica precipitation further, we assumed that the most common water temperature for the impact-generated as well as the volcanic heat-induced hydrothermal activity lies around 150 °C, extracted the fluid from our reaction at this temperature and a W/R of 1, and cooled that fluid to 1 °C. This precipitated 0.35 g of minerals, divided into 99.96 wt% SiO_2 with 0.04 wt% fluorite and traces of pyrite. This demonstrates that a two-step alteration is capable of precipitating pure silica, which in turn makes it appear likely that cooling of any higher T alteration fluid could be responsible for pure SiO_2 precipitation observed around Home Plate. Such higher temperatures could have further enhanced fluid flow. Considering that multiple events (cf. Fig. 6) might have remobilized fluid and leached deposits from prior alteration events, purification of silica by such a two-step process seems likely, but cannot rule out any acidic scenario.

Mg-Fe Carbonates

Carbonates have been found by Spirit in the Comanche outcrop (Morris et al. 2010). The carbonate composition is given as magnesite dominated with 25% of Fe-carbonate, which is similar to the ALH 84001 carbonates (e.g., Harvey and McSween 1996; Bridges and Grady 2000). From orbit Mg-and Fe, carbonates have been observed as well (Carter and Poulet 2012), and the Comanche outcrop looks somewhat similar to phyllosilicate outcrops (cf. figs. 2b and 3 of Carter and Poulet 2012, for example) suggesting that both could be linked to hydrothermal alteration along fractures. The high abundance of carbonates (approximately 26 wt%; Morris et al. 2010) suggests pervasive alteration under high CO_2 partial pressure. Morris and co-workers execute a mass balance calculation assuming that all FeO, MgO, MnO, and CaO is bound in carbonates. This leaves a "residue" high in SiO_2, Al_2O_3, and Fe_2O_3, but also SO_3. This is in agreement with our models at epithermal conditions (Fig. 2), where carbonate formation is accompanied by kaolinite and a SiO_2-phase, which are both invisible to the Mössbauer instrument, but amorphous SiO_2 has been detected alongside the carbonates by Mini-TES (Morris et al. 2010).
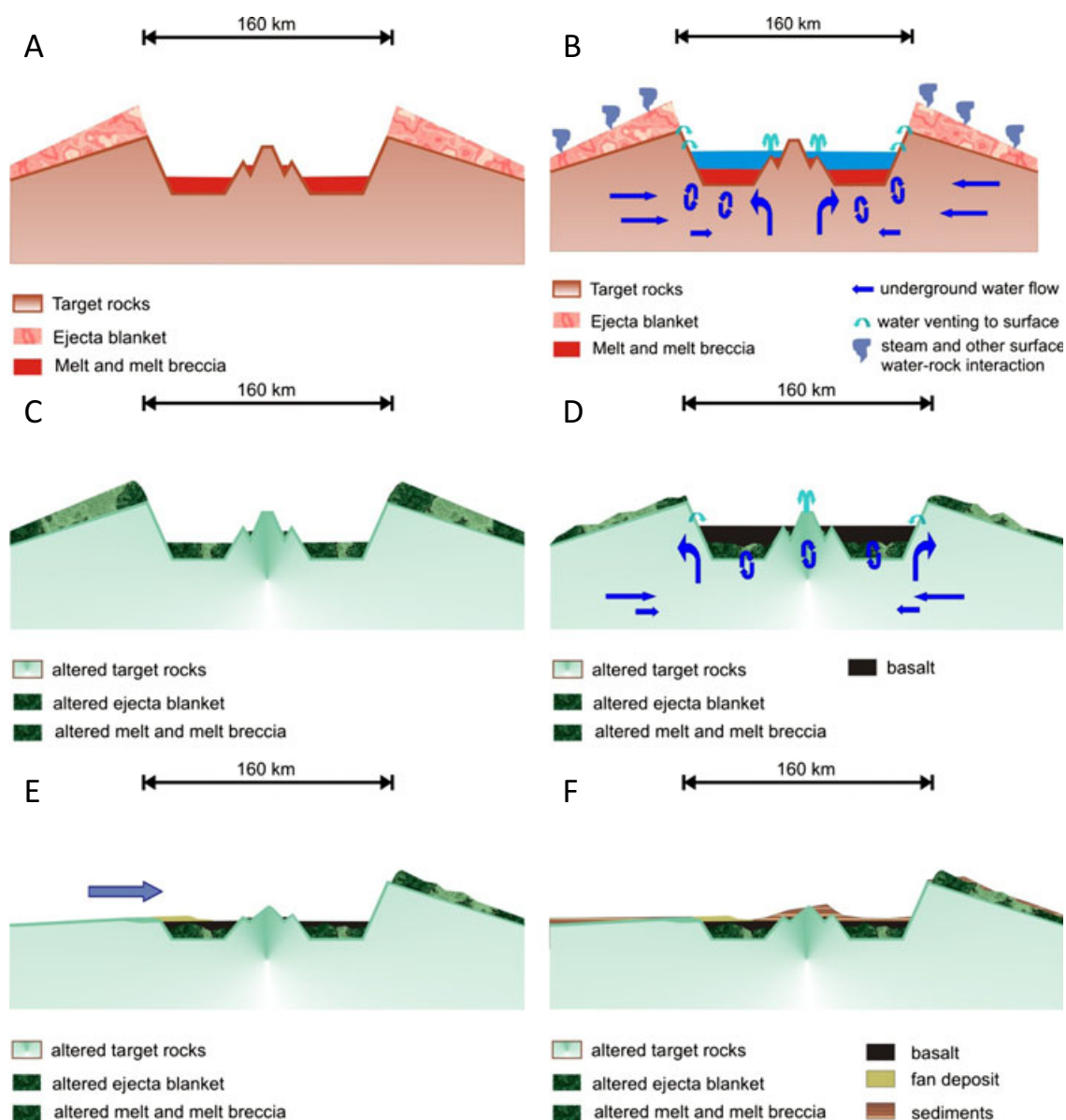
Fig. 6. The fluid history of Gusev crater in relation to impact, volcanism, and fluvial activity. A) 160 km diameter Gusev crater after the impact with hot/molten rock in the crater moat and the ejecta blanket. Additional heat comes from the central uplift. B) In the presence of water, a hydrothermal system is initiated (see text), especially taking advantage of the fractured zones around and in the central uplift and at the inner crater walls. C) Hydrothermal activity is most intense in the central uplift and the inner crater walls, while hot hydrous alteration is prominent in the ejecta blanket and the melt sheet in the crater moat. D) Later heating during volcanic activity has the capability of renewing the hydrothermal activity, taking advantage of pre-existing fractures and pathways. E) Fluvial activity breaches the rim, thereby transporting in pre-altered material eroded from the crater rim, but also offering a new opportunity for hydrous alteration, i.e., weathering. F) Finally, (eolian) sediments are deposited.

Phyllosilicates

A mineralogical survey of Gusev crater by Carter and Poulet (2012) revealed phyllosilicates in the Columbia Hills and in fluvial-lacustrine sediments to the southeast of the Columbia Hills. In addition, montmorillonite has been detected by APXS and Mössbauer (Clark et al. 2007). These phyllosilicates may not be related to the alteration mineralogy seen at Home Plate and surrounding region; however, the results of our models can be used to constrain the conditions of their formation. Therefore, we include a description here as well.

The Fe-Mg (and not pure Fe) nature of the phyllosilicate matches our nontronite chemistry $(Fe_2Mg_{0.165}(AlSi_3O_{10})(OH)_2)$. As no chlorite is reported,

this narrows the range of formation conditions to a carbon dioxide-poor, intermediate-temperature regime. In our 150 °C model, W/R of intermediate-high between 2000 and 1000 allow for nontronite precipitation with minor kaolinite and no chlorite. This can explain the occurrences of Fe/Mg-phyllosilicates in the Columbia Hills, but the fluvial-lacustrine sediments show Fe/Mg-phyllosilicates together with Al-phyllosilicate signatures (halloysite/kaolinite; Carter and Poulet 2012), indicating higher W/R than pure nontronite (Fig. 2). Montmorillonite has also been considered for the independence-class rocks at Husband Hill in the Columbia Hills based on the bulk chemistry of the outcrop (Clark et al. 2007). The independence-class rocks, presumably montmorillonite or similar smectite, analyzed is iron-poor (with approximately 4 wt% FeO) with high Al/Si ratios. However, infrared spectroscopy does not indicate the presence of crystalline smectite, but is suggestive of an Al-rich phyllosilicate (Clark et al. 2007). Such Al-rich phyllosilicate compositions are consistent with our 150 °C model, but higher W/R than for a deposit with nontronite, but no Al-rich phyllosilicate.

The phyllosilicates could have been formed at epithermal conditions either in the volcanic systems of the Southern Highlands or in the crater rim during the postimpact hydrothermal phase of Gusev, and be subsequently eroded and transported into the crater by the Ma'am Vallis fluvial activity breaching the rim. But nontronite formation is also possible under neutral weathering conditions (Chevrier et al. 2007), which makes in situ formation of the phyllosilicates in the fluvial units by weathering of sediments of basaltic mineralogy and chemistry a third option to consider.

IMPLICATIONS FOR THE FORMATION OF ALTERATION PHASES IN GUSEV CRATER

Bulk chemical data of the Home Plate outcrop support the assumption of high- and low-temperature aqueous alteration because elements more susceptible to alteration show correlations with mineralogy and stratigraphic position within the Home Plate sequence (Schmidt et al. 2008, 2009). However, assessing formation conditions of alteration phases starts with understanding their geologic context. The crater morphology, mineralogy, and geochemistry of Gusev crater observed today are the consequence of impact crater formation, volcanic activity, fluvial activity, and sedimentation. To understand the alteration mineralogy seen at Home Plate and surrounding Columbia Hills, we will combine the calculated alteration mineralogy from our models, the alteration mineralogy seen by

MER Spirit, and the geologic context of these minerals and place constraints on the formation conditions of alteration mineralogy within Gusev crater.

Impact Crater Formation

Our discussion of the geologic history of Gusev crater begins with the formation of the impact crater (Fig. 6A), which is an approximately 160 km diameter, Noachian in age, impact crater located on the dichotomy boundary between the southern highlands and the northern lowlands near large volcanic domes such as Apollinaris Patera (Squyres et al. 2006). Its rim is variable in height, with the greatest heights occurring to the east and southeast. The present-day relief difference between the highest parts of the rim and the crater floor in the same quadrangle exceeds 2600 m for the highest points of the rim compared with the floor.

If the Columbia Hills are part of the central uplift of Gusev or from mutual interference of overlapping crater rims (McCoy et al. 2008; Parker et al. 2010), the observed minerals could be generated through post-impact hydrothermal processes (Fig. 6B). Immediately after the impact, temperatures underneath the crater center exceeded 1000 °C and in the presence of subsurface water would have initiated a long-lived hydrothermal system under the crater structure with upwelling water in the central uplift and outflow from the inner crater wall fractures of the rim (Abramov and Kring 2005). While the Abramov and Kring (2005) calculations assume an above-freezing surface temperature, models of impact-cratering into ice-bearing targets result in lower temperatures below the central peak (approximately 625 °C), but still find a hot-water environment under the highly fractured central uplift and ice to be thawing as far from the crater center as the rim (Ivanov and Pierazzo 2011). Independent of surface temperatures at the time of the impact, a long-lived hydrothermal system underneath the central uplift of Gusev appears to be likely, and Abramov and Kring (2004) predicted SiO_2-phases, carbonates, and hematite to be found by Spirit. While the hydrothermal activity will have altered the subsurface, at the same time hot hydrous alteration occurred in the cooling melt sheet in the crater moat and in the ejecta blanket outside the crater (Fig. 6C). Those systems would cool from the highest to ambient temperature and produce a range of alteration phases, as shown in our models. During cooling, high-temperature phases are mostly overprinted. Therefore, the most frequently observed phases are those formed in the intermediate temperature range, i.e., the phyllosilicates kaolinite, nontronite, chlorite, and serpentine, depending on W/R (Fig. 2). The mineral formation is accompanied by a chlorine

and silica-rich brine (Fig. 4), which can subsequently be separated from the site of initial alteration and deposit silica upon cooling and/or evaporation (Fig. 5). If—instead of being the central uplift of Gusev—the Columbia Hills were produced by overlapping crater rims, i.e., a double impact (McCoy et al. 2008), depending on the age difference of the two, the second impact might have hit terrain with an increased geothermal gradient, but will certainly have impacted a prefractured target. Overall temperature regimes might have been lower than in the central uplift case, but fluid flow would still be likely.

Volcanic Activity—Lava Plains and Pyroclastic Activity

The geologic history of Gusev continues past the initial impact crater-forming stage, providing further opportunities for the formation of alteration mineralogy. Volcanic activity is seen in Gusev crater at the lava plains around the Columbia Hills, the volcanic rocks (including the scoriaceous Irvine Class rocks) in the Columbia Hills, and the Home Plate plateau in the Columbia Hills (Fig. 6D), which could have triggered a new generation of hydrothermal alteration.

The lava plains of Gusev crater were well studied from orbit even before MER Spirit landed and were revealed to be basaltic in nature, thought to be Hesperian in age, postdate older floor materials, and are concurrent with volcanic activity at nearby Apollinaris Patera (Greeley et al. 2005; Golombek et al. 2006; Kerber et al. 2011). The Spirit rover investigated some of these rocks, which became deemed the Adirondack-class basalts (McSween et al. 2004). The liquidus temperature of the Adirondack-class basalt Humphrey at 1bar is approximately 1275–1300 °C (Monders et al. 2007; Filiberto et al. 2008). Their mineralogy, specifically the ≤25% olivine with minor pyroxene, feldspar, and basaltic glass (McSween et al. 2004, 2008), is consistent with eruption and cooling significantly below the liquidus temperature before quenching of the lava at <1200 °C (75–100 °C below the liquidus based on experimental results; Filiberto et al. 2008; Monders et al. 2007). Taking typical cooling rates for Martian magmas (0.03–3 °C h^{-1}; Mikouchi et al. 1998, 1999, 2001, 2004), we calculate cooling times of 400–40,000 h. However, this does not take into account lava flow thickness or volume, so these should be taken as minimum cooling times. Eruptions not only provide heat to the surrounding regions but they also provide H_2O, CO_2, S, Cl, F, etc. (e.g., Webster 1990, 1997; Dixon et al. 1991). As shown above, Martian magmas can contain up to 0.5 wt% CO_2 prior to eruption, with the solubility of water in magmas significantly higher than that of CO_2 (e.g., Dixon and Stolper 1995).

Therefore, Adirondack-class basalts could have provided significant quantities of water to the surrounding regions, assuming that they were hydrous magmas. In addition, Martian magmas are thought to be rich in halogens and sulfur (e.g., Dreibus and Wänke 1985; Filiberto and Treiman 2009; Righter et al. 2009; Patiño Douce et al. 2011). Therefore, upon eruption, Adirondack class basalts would have provided heat and CO_2-, halogen-, and sulfur-rich fluids to the surrounding area that would be available for hydrothermal alteration. In the presence of subsurface water, heat from eruption would have initiated short-lived hydrothermal systems with upwelling water in similar places to the impact crater scenario (Fig. 6D). In addition, localized hydrothermal activity would have occurred from eruption and degassing of the magma and interaction of this degassed fluid with the crust.

Another stage of volcanic activity in Gusev crater is seen at the Home Plate outcrop in the Columbia Hills. It is a layered sequence of clastic rocks with alkali basaltic composition, which is interpreted to represent a hydrothermally altered pyroclastic deposit based on textural and chemical analyses (Squyres et al. 2007; Lewis et al. 2008; Schmidt et al. 2008). Texturally, the lower unit of Home Plate indicates that it was deposited in an explosive volcanic setting. An approximately 4 cm bomb sag was found within this unit, which indicates that the clast was ejected from a volcanic vent, and emplaced ballistically into deformable materials (Squyres et al. 2007). On Earth, such deposits occur where the deformable materials were wet at time of eruption. This may suggest the presence of a subsurface hydrologic reservoir during the eruption (Squyres et al. 2007; Lewis et al. 2008). Furthermore, on Earth, explosive eruptions producing pyroclastic deposits require the presence of dissolved volatiles (typically H_2O and CO_2) to drive the eruption (e.g., Wilson 1980; Papale and Polacci 1999; Wallace 2003). Therefore, the eruption that produced the Home Plate outcrop and surrounding basalts in the Inner Basin would have provided significant H_2O and CO_2 to the surrounding region, as well as heat from the eruption, to generate hydrothermal activity. The temperature of this released fluid would be dependent on the eruption temperature. The liquidus at 1bar for the Fastball composition is approximately 1400 °C (Filiberto et al. 2010). Considering that the Home Plate outcrop is dominantly basaltic glass (approximately 45%) with pyroxene and minor olivine and plagioclase (Squyres et al. 2007), the eruption took place just below the 1bar liquidus temperature. Therefore, degassing fluids from the eruption would provide significant heat as well as CO_2 to the surrounding system. The heat released from a pyroclastic eruption would be more localized than from

the basalt flows, but with a more centralized heat and fluid source hydrothermal activity may have been more intense than from a basalt flow. However, we do not know the exact source region for the Home Plate deposit (Wilson and Head 2007) and if the source was not local, the temperature of the deposit would be significantly lower than the calculated value.

Terrestrial magmatic-driven hydrothermal activity produces a wide range of alteration mineralogy depending on the temperature, pressure, parental rock type, permeability of the host rock, the fluid composition, and duration of activity (e.g., Browne 1978). Similar to the results here, typical alteration phases include quartz, kaolinite, montmorillonite, chlorite, as well as many others, depending on location and formation conditions. Temperature estimates for these deposits are typically below 280 °C, but some have reported a maximum temperature just above 300 °C. So the conditions of our results that produced a chlorite–serpentine–quartz assemblage with either magnetite or epidot–garnet–pyroxene–feldspar at high and low W/R, respectively (Fig 1), are directly comparable to those in terrestrial magmatic hydrothermal activity.

Fluvial Activity and Sedimentation

Finally, sedimentation has occurred providing another time for alteration mineralogy formation (Fig. 6E). We discuss sedimentation last, but sedimentation presumably began shortly after the formation of the impact crater (Cabrol 2008; Crumpler et al. 2011). Spirit found neither the nature nor ubiquity of sediments that were expected from the fact that Gusev crater is the catchment area for Ma'am Vallis (Kuzmin et al. 2004). Instead, the rover found itself on a basaltic plain with the only sediments being soil made of wind-blown Martian dust (Squyres et al. 2004a; Cabrol 2008). There are, however, orbital observations of phyllosilicate minerals (Clark et al. 2007; Carter and Poulet 2012). The observations reveal Mg-bearing saponite (or Fe-Mg-vermiculite, which is considered less likely by the authors; Carter and Poulet 2012). This observation is matched by our models at 150 °C and 13 °C; thus we can exclude high-T alteration, but the detection of only one phase does not distinguish between the epithermal and weathering/lacustrine scenarios. At two locations in the fluvial-lacustrine deposit, kaolinite is detected, which implies a higher water-to-rock ratio than the saponite. Finally, airborne sedimentation occurred (Cabrol 2008; Crumpler et al. 2011; Fig. 6F), which could redistribute alteration phases, but no new phases are likely to be formed there.

CONCLUSIONS

Gusev crater is a large, Noachian impact basin, in which multiple episodes of hydrothermal alteration have been possible. Impact-generated hydrothermal alteration would have been the first phase, ranging from highest temperatures to ambient upon cooling of the system. Volcanism and infill of the crater by basaltic lavas provided another intense heating event probably associated with hydrothermal activity. Weathering could have further modified primary rocks and existing alteration assemblages through transport; physical weathering; and chemical, low-T hydrous alteration.

Alteration assemblages formed by those events depend on temperature and water availability during the hydrothermal activity. At high temperatures (300 °C), magnetite occurs at very high W/R ratios, but the alteration assemblage is dominated by chlorite and serpentine over most of the W/R range. Quartz, epidote, and typical high-T phases such as feldspar, pyroxene, and garnet occur at low W/R. At epithermal temperatures (150 °C), hematite occurs at very high W/R. A range of phyllosilicates, including kaolinite, nontronite, chlorite, and serpentine are precipitated at specific W/R. Amphibole, with garnet, feldspar, and pyroxene occur at low W/R. If the CO_2 content of the system is high, the assemblage is dominated by carbonate with increasing amounts of an SiO_2-phase, kaolinite, carpholite, and chlorite with lower W/R. At temperatures of hydrous weathering (13 °C), the oxide phase is goethite, silicates are chlorite, nontronite, and talc, plus an SiO_2-phase. In the presence of CO_2, the mineral assemblage at high W/R remains the same, and only at low W/R, i.e., with increasing salinity, carbonate precipitates.

The geochemical gradients observed at Home Plate are attributed to short-lived, initially high (300 °C) temperature, but fast cooling events (Schmidt et al. 2009), which are in agreement with our models and our interpretation of a multistage alteration scenario of Home Plate and Gusev in general. The succession of potential water-based alteration events in Gusev crater is important for the investigation of habitability, because it repeatedly offers habitable environments over a large time span. Wall rock alteration at various temperatures and during different geological processes within Gusev crater has two effects, both of which increase the habitability of the local environment: precipitation of hydrous sheet silicates, and formation of a brine, which might contain elements essential for life in diluted, easily accessible form. Although it certainly depends on a complex set of factors if life could ever have used any of the habitable environments (Cockell et al. 2012), the succession of events will have enhanced opportunities and

prolonged the lifetime of habitability, especially for species that possess the ability to endure adverse conditions in a dormant or spore state.

Editorial Handling—Dr. Christine Floss

REFERENCES

Abramov O. and Kring D. A. 2004. Impact-generated hydrothermal activity at Gusev crater: Implications for the Spirit mission (abstract #1976). 35th Lunar and Planetary Science Conference. CD-ROM.

Abramov O. and Kring D. A. 2005. Impact-induced hydrothermal activity on early Mars. *Journal of Geophysical Research* 110:E12S09.

Allen C. C., Gooding J. L., and Keil K. 1982. Hydrothermally altered impact melt rock and breccia: Contributions to the soil of Mars. *Journal of Geophysical Research* 87:10083–10101.

Arvidson R. E., Ruff S., Morris R. V., Ming D., Crumpler L., Yen A., Squyres S., Bell J. F., Cabrol N., Clark B. C., Farrand W., Gellert R., Greenberger R., Grant J., Guinness E. A., Herkenhoff K. E., Hurowitz J. A., Johnson J. R., Klingelhoefer G., Lewis K. W., Li R., McCoy T., Moersch J., McSween H. Y., Murchie S. L., Schmidt M., Schröder C., Wang A., Wiseman S., Madsen M. B., Goetz W., and McLennan S. 2008. Spirit Mars Rover Mission to the Columbia Hills, Gusev crater: Mission overview and selected results from the Cumberland Ridge to Home Plate. *Journal of Geophysical Research* 113:E12S33. doi:10.1029/2008JE003183.

Arvidson R. E., Bell J. F., III, Bellutta P., Cabrol N. A., Catalano J. G., Cohen J., Crumpler L. S., Des Marais D. J., Estlin T. A., Farrand W. H., Gellert R., Grant J. A., Greenberger R. N., Guinness E. A., Herkenhoff K. E., Herman J. A., Iagnemma K. D., Johnson J. R., Klingelhöfer G., Li R., Lichtenberg K. A., Maxwell S. A., Ming D. W., Morris R. V., Rice M. S., Ruff S. W., Shaw A., Siebach K. L., de Souza P. A., Stroupe A. W., Squyres S. W., Sullivan R. J., Talley K. P., Townsend J. A., Wang A., Wright J. R., and Yen A. S. 2010. Spirit Mars Rover Mission: Overview and selected results from the northern Home Plate Winter Haven to the side of Scamander crater. *Journal of Geophysical Research* 115:E00F03.

Arvidson R. E., Ashley J. W., Bell J. F., III, Chojnacki M., Cohen J., Economou T. E., Farrand W. H., Fergason R., Fleischer I., Geissler P., Gellert R., Golombek M. P., Grotzinger J. P., Guinness E. A., Haberle R. M., Herkenhoff K. E., Herman J. A., Iagnemma K. D., Jolliff B. L., Johnson J. R., Klingelhöfer G., Knoll A. H., Knudson A. T., Li R., McLennan S. M., Mittlefehldt D. W., Morris R. V., Parker T. J., Rice M. S., Schröder C., Soderblom L. A., Squyres S. W., Sullivan R. J., and Wolff M. J. 2011. Opportunity Mars Rover Mission: Overview and selected results from Purgatory ripple to traverses to Endeavour crater. *Journal of Geophysical Research* 116:E00F15.

Bandura A. V. and Lvov S. N. 2006. The ionization constant of water over wide ranges of temperature and density. *Journal of Physical and Chemical Reference Data* 35:15–30.

Barnes H. L. 1997. *Geochemistry of hydrothermal ore deposits*, 3rd ed. Hoboken, New Jersey: John Wiley and Sons.

Berger G., Toplis M. J., Treguir E., D'Uston C., and Pinet P. 2009. Evidence in favour of small amounts of ephemeral and transient water during alteration at Meridiani Planum, Mars. *American Mineralogist* 94:1279–1282.

Van Berk W. and Fu Y. 2012. Reproducing hydrogeochemical conditions triggering the formation of carbonate and phyllosilicate alteration mineral assemblages on Mars (Nili Fossae region). *Journal of Geophysical Research* 116. doi:10.1029/2011JE003886, 16 p.

Bibring J.-P., Langevin Y., Mustard J. F., Poulet F., Arvidson R., Gendrin A., Gondet B., Mangold N., Pinet P., Forget F., The Omega team: Berthe M., Bibring J.-P., Gendrin A., Gomez C., Gondet B., Jouglet D., Poulet F., Soufflot A., Vincendon M., Combes M., Drossart P., Encrenaz T., Fouchet T., Merchiorri R., Belluci G., Altieri F., Formisano V., Capaccioni F., Cerroni P., Coradini A., Fonti S., Korablev O., Kottsov V., Ignatiev N., Moroz V., Titov D., Zasova L., Loiseau D., Mangold N., Pinet P., Doute S., Schmitt B., Sotin C., Hauber E., Hoffmann H., Jaumann R., Keller U., Arvidson R., Mustard J. F., Duxbury T., Forget F., and Neukum G. 2006. Global mineralogical and aqueous Mars history derived from OMEGA/Mars Express data. *Science* 312:400–404.

Bridges J. C. and Grady M. M. 2000. Evaporite minerals assemblages in the nakhlite (Martian) meteorites. *Earth and Planetary Science Letters* 176:267–279.

Bridges J. C. and Schwenzer S. P. 2012. The nakhlite hydrothermal brine on Mars. *Earth and Planetary Science Letters* 359–360:117–123.

Browne P. 1978. Hydrothermal alteration in active geothermal fields. *Annual Review of Earth and Planetary Sciences* 6:229–250.

Cabrol N. A. 2008. Soil sedimentology at Gusev crater from Columbia memorial station to Winter Haven. *Journal of Geophysical Research* 113:E06S05. doi:10.1029/2007JE002953.

Carter J. and Poulet F. 2012. Orbital identification of clays and carbonates in Gusev crater. *Icarus* 219:250–253.

Changela H. G. and Bridges J. C. 2010. Alteration assemblages in the nakhlites: Variation with depth on Mars. *Meteoritics & Planetary Science* 45:1847–1867.

Chevrier V., Poulet F., and Bibring J.-P. 2007. Early geochemical environment of Mars as determined from thermodynamics of phyllosilicates. *Nature* 448:60–63.

Clark B. C., Arvidson R. E., Gellert R., Morris R. V., Ming D. W., Richter L., Ruff S. W., Michalski J. R., Farrand W. H., Yen A., Herkenhoff K. E., Li R., Squyres S. W.,

Schröder C., Klingelhöfer G., and Bell J. F. 2007. Evidence for montmorillonite or its compositional equivalent in Columbia Hills, Mars. *Journal of Geophysical Research: Planets* 112:E06S01. doi:10.1029/2006je002756.

Cockell C. S., Balme M., Bridges J. C., Davila A., and Schwenzer S. P. 2012. Uninhabited habitats on Mars. *Icarus* 217:184–193. doi:10.1016/j.icarus.2011.10.025.

Cornell R. M. and Schwertmann U. 2003. *The iron oxides. Structure, properties, reactions, occurrences and uses.* Hoboken, New Jersey: Wiley. 663 p

Crumpler L. S., Arvidson R. E., Squyres S. W., McCoy T., Yingst A., Ruff S., Farrand W., McSween Y., Powell M., Ming D. W., Morris R. V., Bell J. F., III, Grant J., Greeley R., DesMarais D., Schmidt M., Cabrol N. A., Heldemann A., Lewis K. W., Wang A. E., Schröder C., Blaney D., Cohen B., Yen A., Farmer J., Gellert R., Guiness E. A., Herkenhoff K. E., Johnson J. R., Klingelhöfer G., McEwen A., Rice J. W., Jr., Rice M., deSouza P., and Hurowitz J. 2011. Field reconnaissance geologic mapping of the Columbia Hills, Mars, based on Mars Exploration Rover Spirit and MRO HiRISE observations. *Journal of Geophysical Research* 116:E00F24. doi:10.1029/2010JE003749.

Diamond L. W. and Akinfiev N. N. 2003. Solubility of CO_2 in water from -1.5 to 100 °C and from 0.1 to 100 MPa: evaluation of literature data and thermodynamic modeling. *Fluid Phase Equilibria* 208:265–290.

Dixon J. E. and Stolper E. M. 1995. An experimental study of water and carbon dioxide solubilities in mid-ocean ridge basaltic liquids. Part II: Applications to degassing. *Journal of Petrology* 36:1633–1646.

Dixon J. E., Stolper E. M., and Clague D. A. 1991. Degassing history of water, sulfur, and carbon in submarine lavas from Kilauea Volcano, Hawaii. *Journal of Geology* 99: 371–394.

Dixon J. E., Stolper E. M., and Holloway J. R. 1995. An experimental study of water and carbon dioxide solubilities in mid-ocean ridge basaltic liquids. *Journal of Petrology* 36:1607–1631.

Dreibus G. and Wänke H. 1985. Mars, a volatile-rich planet. *Meteoritics* 20:367–381.

Filiberto J. and Dasgupta R. 2011. Fe^{2+}-Mg partitioning between olivine and basaltic melts: Applications to genesis of olivine-phyric shergottites and conditions of melting in the Martian interior. *Earth and Planetary Science Letters* 304:527–537.

Filiberto J. and Treiman A. H. 2009. Martian magmas contained abundant chlorine, but little water. *Geology* 37:1087–1090.

Filiberto J., Treiman A. H., and Le L. 2008. Crystallization experiments on a Gusev Adirondack basalt composition. *Meteoritics & Planetary Science* 43:1137–1146.

Filiberto J., Dasgupta R., Kiefer W. S., and Treiman A. H. 2010. High pressure, near-liquidus phase equilibria of the Home Plate basalt Fastball and melting in the Martian mantle. *Geophysical Research Letters* 37:L13201. doi:10.1029/12010GL043999.

Gleason J. D., Kring D. A., Hill D. H., and Boyton W. V. 1997. Petrography and bulk chemistry of Martian orthopyroxenite ALH 84001: Implications for the origin of secondary carbonates. *Geochimica et Cosmochimica Acta* 61:3503–3512.

Golombek M. P., Crumpler L. S., Grant J. A., Greeley R., Cabrol N. A., Parker T. J., Rice J. W. Jr., Ward J. G., Arvidson R. E., Moersch J. E., Fergason R. L., Christensen P. R., Castaño A., Castaño R., Haldemann A. F. C., Li R., Bell J. F. III, and Squyres S. W. 2006. Geology of the Gusev cratered plains from the Spirit rover transverse. *Journal of Geophysical Research* 111:E02S07. doi:10.1029/2005je002503.

Goodrich C. A., Herd C. D. K., and Taylor L. A. 2003. Spinels and oxygen fugacity in olivine-phyric and lherzolitic shergottites. *Meteoritics & Planetary Science* 38:1773–1792.

Greeley R., Foing B. H., McSween H. Y., Neukum G., Pinet P., van Kan M., Werner S. C., Williams D. W., and Zegers T. E. 2005. Fluid lava flows in Gusev crater, Mars. *Journal of Geophysical Research* 110:E05008. doi:10.1029/2005JE002401.

Griffith L. L. and Shock E. L. 1995. A geochemical model for the formation of hydrothermal carbonates on Mars. *Nature* 377:406–408.

Griffith L. L. and Shock E. L. 1997. Hydrothermal hydration of Martian crust: Illustration via geochemical model calculations. *Journal of Geophysical Research* 102:9135–9143.

Hagerty J. J. and Newsom H. E. 2003. Hydrothermal alteration at the Lonar Lake impact structure, India: Implications for impact cratering on Mars. *Meteoritics & Planetary Science* 38:365–381.

Hallis L. J. and Taylor G. J. 2011. Comparisons of the four Miller Range nakhlites, MIL 03346, 090030, 090032 and 090136: Textural and compositional observations of primary and secondary mineral assemblages. *Meteoritics & Planetary Science* 46:1787–1803.

Harvey R. P. and McSween H. Y., Jr. 1996. A possible high-temperature origin for the carbonates in the Martian meteorite ALH 84001. *Nature* 382:49–51.

Herd C. D. K. 2003. The oxygen fugacity of olivine-phyric Martian basalts and the components within the mantle and crust of Mars. *Meteoritics & Planetary Science* 38:1793–1805.

Herd C. D. K., Borg L. E., Jones J. H., and Papike J. J. 2002. Oxygen fugacity and geochemical variations in the Martian basalts: Implications for Martian basalt petrogenesis and the oxidation state of the upper mantle of Mars. *Geochimica et Cosmochimica Acta* 66:2025–2036.

Hicks L. J., Bridges J. C., and Gurman S. J. 2012. Ferric content of nakhlite hydrothermal minerals (abstract #2253). 43rd Lunar and Planetary Science Conference. CD-ROM.

Hirschmann M. M. and Withers A. C. 2008. Ventilation of CO2 from a reduced mantle and consequences for the early Martian greenhouse. *Earth and Planetary Science Letters* 270:147–155.

Ivanov B. A. and Pierazzo E. 2011. Impact cratering in H2O-bearing targets on Mars: Thermal field under craters as starting conditions for hydrothermal activity. *Meteoritics & Planetary Science* 46:601–619.

Kerber L., Head J. W., Madeleine J.-B., Forget F., and Wilson L. 2011. The dispersal of pyroclasts from Apollinaris Patera, Mars: Implications for the origin of the Medusae Fossae Formation. *Icarus* 216:212–220.

Kirschvink J. L., Maine A. T., and Vali H. 1997. Paleomagnetic evidence of a low-temperature origin of carbonate in the Martian meteorite ALH 84001. *Science* 275:1629–1633.

Kring D. A., Swindle T. D., Gleason J. D., and Grier J. A. 1998. Formation and relative ages of maskelynite and carbonate in ALH 84001. *Geochimica et Cosmochimica Acta* 62:2155–2166.

Kuzmin R. O., Greeley R., Landheim R., Cabrol N. A., and Farmer J. D. 2004. Geologic map of the MTM–15182 and MTM–15187 quadrangles, Gusev crater–Ma'adim Vallis Region, Mars. U.S. Geological Survey. Available at http://pubs.usgs.gov/imap/i2666/.

Lee M. R., Tomkinson T., Mark D. F., Stuart F. M., and Smith C. L. 2013. Evidence for silicate dissolution on Mars from the Nakhla meteorite. *Meteoritics & Planetary Science* 48:228–240. doi:10.1111/maps.12053.

Lewis K. W., Aharonson O., Grotzinger J. P., Squyres S. W., Bell J. F., III, Crumpler L. S., and Schmidt M. E. 2008. Structure and stratigraphy of Home Plate from the Spirit Mars Exploration Rover. *Journal of Geophysical Research* 113:E12S36. doi:10.1029/2007je003025.

Mangold N., Carter J., Poulet F., Dehouck E., Ansan V., and Loizeau D. 2012. Late Hesperian aqueous alteration at Majuro crater, Mars. *Planetary and Space Science* 72:18–30.

Marion G. M., Catling D. C., Crowley J. K., and Kargel J. S. 2011. Modeling hot spring chemistries with applications to Martian silica formation. *Icarus* 212:629–642.

Marzo G. A., Davila A. F., Tornabene L. L., Dohm J. M., Fairén A. G., Gross C., Kneissl T., Bishop J. L., Roush T. L., and McKay C. P. 2010. Evidence for Hesperian impact-induced hydrothermalism on Mars. *Icarus* 208:667–683.

McAdam A. C., Zolotov M. Y., Mironenko M. V., and Sharp T. G. 2008. Formation of silica by low-temperature acid alteration of Martian rocks: Physical-chemical constraints. *Journal of Geophysical Research* 113:E08003.

McCoy T., Sims M., Schmidt M. E., Edwards L., Tornabene L. L., Crumpler L. S., Cohen B. A., Soderblom L. A., Blaney D. L., Squyres S. W., Arvidson R. E., Rice J. W., Treguier E., d'Uston C., Grant J. A., McSween H. Y., Golombek M. P., Haldemann A. F. C., and de Souza P. A. 2008. Structure, stratigraphy, and origin of Husband Hill, Columbia Hills, Gusev crater, Mars. *Journal of Geophysical Research* 113:E06S03. doi: 10.1029/2007JE 003041.

McCubbin F. M., Tosca N. J., Smirnov A., Nekvasil H., Steele A., Fries M., and Lindsley D. H. 2009. Hydrothermal jarosite and hematite in a pyroxene-hosted melt inclusion in Martian meteorite Miller Range (MIL) 03346: Implications for magmatic-hydrothermal fluids on Mars. *Geochimica et Cosmochimica Acta* 73:4907–4917.

McLennan S., Bell J. F., Calvin W. M., Christensen P. R., Clark B. C., De Souza P. A., Farmer J. D., Farrand W., Fike D. A., Gellert R., Ghosh A., Glotch T. D., Grotzinger G., Knoll A. H., Learner Z., Malin M., McSween H. Y., Pocock J., Ruff S. W., Soderblom L., Squyres S. W., Tosca N. J., Watters W. A., Wyatt M. B., and Yen A. 2005. Provenance and diagenesis of the evaporite-bearing Burns formation, Meridiani Planum, Mars. *Earth and Planetary Science Letters* 240:95–121.

McSween H. Y. and Treiman A. H. 1998. Chondritic meteorites. In *Martian meteorites*, edited by Papike J. J. Reviews in Mineralogy, vol. 36. Washington, D.C.: Mineralogical Society of America. pp. 6-01–06-40.

McSween H. Y., Arvidson R. E., Bell J. F., Blaney D., Cabrol N. A., Christensen P. R., Clark B. C., Crisp J. A., Crumpler L. S., Des Marais D. J., Farmer J. D., Gellert R., Ghosh A., Gorevan S., Graff T., Grant J., Haskin L.

A., Herkenhoff K. E., Johnson J. R., Jolliff B. L., Klingelhoefer G., Knudson A. T., McLennan S., Milam K. A., Moersch J. E., Morris R. V., Rieder R., Ruff S. W., de Souza P. A., Squyres S. W., Wanke H., Wang A., Wyatt M. B., Yen A., and Zipfel J. 2004. Basaltic rocks analyzed by the Spirit Rover in Gusev crater. *Science* 305:842–845.

McSween H. Y., Wyatt M. B., Gellert R., Bell J. F., Morris R. V., Herkenhoff K. E., Crumpler L.S., Milam K. A., Stockstill K. R., Tornabene L. L., Arvidson R. E., Bartlett P., Blaney D., Cabrol N. A., Christensen P. R., Clark B. C., Crisp J. A., Des Marais D. J., Economou T., Farmer J. D., Farrand W., Ghosh A., Golombek M., Gorevan S., Greeley R., Hamilton V. E., Johnson J. R., Joliff B. L., Klingelhöfer G., Knudson A. T., McLennan S., Ming D., Moersch J. E., Rieder R., Ruff S. W., Schröder C., de Souza P. A., Squyres S. W., Wänke H., Wang A., Yen A., and Zipfel J. 2006. Characterization and petrologic interpretation of olivine-rich basalts at Gusev crater, Mars. *Journal of Geophysical Research-Planets* 111:EO2510. doi: 10.1029/2005E02477.

McSween H. Y., Ruff S. W., Morris R. V., Gellert R., Klingelhöfer G., Christensen P. R., McCoy T., Ghosh A., Moersch J. E., Cohen B. A., Rogers A. D., Schroder C., Squyres S., Crisp J., and Yen A. 2008. Mineralogy of volcanic rocks in Gusev crater, Mars: Reconciling Mössbauer, APXS, and Mini-TES spectra. *Journal of Geophysical Research-Planets* 133:E06S04. doi:10.1029/ 2007JE002970.

McSween H. Y., Taylor G. J., and Wyatt M. B. 2009. Elemental composition of the Martian crust. *Science* 324:736–739.

Meyer C. 2010. *Mars Meteorite Compendium; JSC #27672 Revision C*. Houston, Texas: Astromaterials Research and Exploration Science (ARES) Johnson Space Center.

Mikouchi T., Miyamoto M., and McKay G. A. 1998. Mineralogy of Antarctic basaltic shergottite QUE 94201: Similarities to EETA7900 1 (Lithology B) Martian meteorite. *Meteoritics & Planetary Science* 33:181–189.

Mikouchi T., Miyamoto M., and McKay G. A. 1999. The role of undercooling in producing igneous zoning trends in pyroxenes and maskelynites among basaltic Martian meteorites. *Earth and Planetary Science Letters* 173:235–256.

Mikouchi T., Miyamoto M., and McKay G. A. 2001. Mineralogy and petrology of the Dar al Gani 476 Martian meteorite: Implications for its cooling history and relationship to other shergottites. *Meteoritics & Planetary Science* 36:531–548.

Mikouchi T., Koizumi E., McKay G., Monkawa A., Ueda Y., Chokai J., and Miyamoto M. 2004. Yamato 980459: Mineralogy and petrology of a new shergottite-related rock from Antarctica. *Antarctic Meteorite Research* 17:13–34.

Ming D. W., Mittlefehldt D. W., Morris R. V., Golden D. C., Gellert R., Yen A., Clark B. C., Squyres S. W., Farrand W. H., Ruff S. W., Arvidson R. E., Klingelhöfer G., McSween H. Y., Rodionov D. S., Schröder C., de Souza P. A., Jr., and Wang A. 2006. Geochemical and mineralogical indicators for aqueous processes in the Columbia Hills of Gusev crater, Mars. *Journal of Geophysical Research* 111:E02S12. doi: 10.1029/2005JE 002560.

Ming D. W., Gellert R., Morris R. V., Arvidson R. E., Brückner J., Clark B. C., Cohen B. A., d'Uston C.,

Economou T., Fleischer I., Klingelhöfer G., McCoy T. J., Mittlefehldt D. W., Schmidt M. E., Schröder C., Squyres S. W., Tréguier E., Yen A. S., and Zipfel J. 2008. Geochemical properties of rocks and soils in Gusev crater, Mars: Results of the alpha particle x-ray spectrometer from Cumberland Ridge to Home Plate. *Journal of Geophysical Research* 113:E12S39. doi:10.1029/2008JE003195.

Minissale A., Vaselli O., Chandrasekharam D., Magro G., Tassi F., and Casiglia A. 2000. Origin and evolution of "intracratonic" thermal fluids from central-western peninsular India. *Earth and Planetary Science Letters* 181:377–394.

Monders A. G., Médard E., and Grove T. L. 2007. Phase equilibrium investigations of the Adirondack class basalts from the Gusev plains, Gusev crater, Mars. *Meteoritics & Planetary Science* 42:131–148.

Morris R. V., Klingelhöfer G., Schröder C., Rodionov D. S., Yen A., Ming D. W., De Souza P. A., Fleischer I., Wdowiak T., Gellert R., Bernhardt B., Evlanov E. N., Zubkov B., Foh J., Bonnes U., Kankeleit E., Gütlich P., Renz F., Squyres S., and Arvidson R. E. 2006. Mössbauer mineralogy of rock, soil, and dust at Gusev crater, Mars: Spirit's journey through weakly altered olivine basalt on the plains and pervasively altered basalt in the Columbia Hills. *Journal of Geophysical Research* 111:E02S13. doi:10.1029/2005JE002584.

Morris R. V., Klingelhöfer G., Schröder C., Fleischer I., Ming D. W., Yen A. S., Gellert R., Arvidson R. E., Rodionov D. S., Crumpler L. S., Clark B. C., Cohen B. A., McCoy T. J., Mittlefehldt D. W., Schmidt M. E., de Souza P. A., Jr, and Squyres S. W. 2008. Iron mineralogy and aqueous alteration from Husband Hill through Home Plate at Gusev crater, Mars: Results from the Mössbauer instrument on the Spirit Mars Exploration Rover. *Journal of Geophysical Research* 113:E12S42. doi:10.1029/2008je003201.

Morris R. V., Ruff S. W., Gellert R., Ming D. W., Arvidson R. E., Clark B. C., Golden D. C., Siebach K., Klingelhöfer G., Schröder C., Fleischer I., Yen A. S., and Squyres S. W. 2010. Identification of carbonate-rich outcrops on Mars by the Spirit Rover. *Science* 329:421–424.

Mustard J. F., Murchie S. L., Pelkey S. M., Ehlmann B. L., Milliken R. E., Grant J. A., Bibring J. P., Poulet F., Bishop J., Dobrea E. N., Roach L., Seelos F., Arvidson R. E., Wiseman S., Green R., Hash C., Humm D., Malaret E., McGovern J. A., Seelos K., Clancy T., Clark R., Marais D. D., Izenberg N., Knudson A., Langevin Y., Martin T., McGuire P., Morris R., Robinson M., Roush T., Smith M., Swayze G., Taylor H., Titus T., and Wolff M. 2008. Hydrated silicate minerals on Mars observed by the Mars CRISM instrument. *Nature* 454:305–309.

Newsom H. E. 1980. Hydrothermal alteration on impact melt sheets with implications for Mars. *Icarus* 44:207–216.

Noguchi T., Nakamura T., Misawa K., Imae N., Aoki T., and Toh S. 2009. Laihunite and jarosite in the Yamato 00 nakhlites: Alteration products on Mars? *Journal of Geophysical Research: Planets* 114:E10004.

Oze C. and Sharma M. 2005. Have olivine, will gas: Serpentinization and the abiogenic production of methane on Mars. *Geophysical Research Letters* 32:L10203.

Palandri J. and Reed M. H. 2004. Geochemical models of metasomtism in ultramafic systems: Serpentinization, rodingization, and sea floor carbonate chimney precipitation. *Geochimica et Cosmochimica Acta* 68:1115–1133.

Papale P. and Polacci M. 1999. Role of carbon dioxide in the dynamics of magma ascent in explosive eruptions. *Bulletin of Volcanology* 60:583–594.

Parker M. v. K., Zegers T., Kneissl T., Ivanov B., Foing B., and Neukum G. 2010. 3D structure of the Gusev crater region. *Earth and Planetary Science Letters* 294:411–423.

Patiño Douce A. E., Roden M. F., Chaumba J., Fleisher C., and Yogodzinski G. 2011. Compositional variability of terrestrial mantle apatites, thermodynamic modeling of apatite volatile contents, and the halogen and water budgets of planetary mantles. *Chemical Geology* 288:14–31.

Reed M. H. 1983. Seawater-basalt reaction and the origin of greenstones and related ore deposits. *Economic Geology* 78:466–485.

Reed M. H. and Palandri J. 2007. Hydrogen produced by reduction of H_2O in rock reaction: Peridotite *vs.* basalt. Proceedings of the 5th International Workshop on Water Dynamics, September 2007, Sendai, Japan. 6 p.

Reed M. H. and Spycher N. F. 2006. *User guide for CHILLER: A program for computing water-rock reactions, boiling, mixing, and other reaction processes in squeous-mineral-gas systems and minplot guide*, 3rd ed. Eugene, Oregon: University of Oregon.

Rice M. S., Bell J. F. III, Cloutis E. A., Wang A., Ruff S. W., Craig M. A., Bailey D. T., Johnson J. R., de Souza P. A., Jr, and Farrand W. H. 2010. Silica-rich deposits and hydrated minerals at Gusev crater, Mars: Vis-NIR spectral characterization and regional mapping. *Icarus* 205:375–395.

Righter K., Pando K., and Danielson L. R. 2009. Experimental evidence for sulfur-rich Martian magmas: Implications for volcanism and surficial sulfur sources. *Earth and Planetary Science Letters* 288:235–243.

Ruff S. W., Farmer J. D., Calvin W. M., Herkenhoff K. E., Johnson J. R., Morris R. V., Rice M. S., Arvidson R. E., Bell J. F. III, Christensen P. R., and Squyres S. W. 2011. Characteristics, distribution, origin, and significance of opaline silica observed by the Spirit Rover in Gusev crater, Mars. *Journal of Geophysical Research* 116:E00F23.

Schmidt M. E., Ruff S. W., McCoy T. J., Farrand W. H., Johnson J. R., Gellert R., Ming D. W., Morris R. V., Cabrol N., and Lewis K. W. 2008. Hydrothermal origin of halogens at Home Plate, Gusev crater. *Journal of Geophysical Research* 113:E06S12. doi:10.1029/2007JE003027.

Schmidt M. E., Farrand W. H., Johnson J. R., Schröder C., Hurowitz J. A., McCoy T. J., Ruff S. W., Arvidson R. E., Des Marais D. J., Lewis K. W., Ming D. W., Squyres S. W., and de Souza P. A. Jr. 2009. Spectral, mineralogical, and geochemical variations across Home Plate, Gusev crater, Mars indicate high and low temperature alteration. *Earth and Planetary Science Letters* 281:258–266.

Schmidt M., Schrader C., and McCoy T. 2011. How oxidized are the Gusev basalts? (abstract #2277). 42nd Lunar and Planetary Science. CD-ROM.

Schwenzer S. P. and Kring D. A. 2009a. Impact-generated hydrothermal alteration on Mars: Clay minerals, oxides,

zeolites, and more (abstract #1421). 40th Lunar and Planetary Science. CD-ROM.

Schwenzer S. P. and Kring D. A. 2009b. Impact-generated hydrothermal systems capable of forming phyllosilicates on Noachian Mars. *Geology* 37:1091–1094.

Schwenzer S. P. and Kring D. A. 2009c. Impact-generated hydrothermal alteration on early Mars in presence of CO_2 (abstract #5262). *Meteoritics & Planetary Science* 44:A188.

Schwenzer S. P. and Kring D. A. 2013. Alteration minerals in impact-generated hydrothermal systems—Exploring host rock variability. *Icarus* 226:487–496.

Schwenzer S. P., Fritz J., Stöffler D., Trieloff M., Amini M., Greshake A., Herrmann S., Herwig K., Jochum K. P., Mohapatra R. K., Stoll B., and Ott U. 2008. Helium loss from Martian meteorites—Mainly induced by shock metamorphism: Evidence from new data and a literature compilation. *Meteoritics & Planetary Science* 43:1841–1859.

Schwenzer S. P., Abramov O., Allen C. C., Bridges J. C., Clifford S. M., Filiberto J., Kring D. A., Lasue J., McGovern P. J., Newsom H. E., Treiman A. H., Vaniman D. T., Wiens R. C., and Wittmann A. 2012a. Gale crater: Formation and post-impact hydrous environments. *Planetary and Space Science* 70:84–95.

Schwenzer S. P., Abramov O., Allen C. C., Clifford S. M., Cockell C. S., Filiberto J., Kring D. A., Lasue J., McGovern P. J., Newsom H. E., Treiman A. H., Vaniman D. T., and Wiens R. C. 2012b. Puncturing Mars: How impact craters interact with the Martian cryosphere. *Earth and Planetary Science Letters* 335–336:9–17.

Squyres S. W., Arvidson R. E., Bell J. F. III, Bruckner J., Cabrol N. A., Calvin W., Carr M. H., Christensen P. R., Clark B. C., Crumpler L., Des Marais D. J., d'Uston C., Economou T., Farmer J., Farrand W., Folkner W., Golombek M., Gorevan S., Grant J. A., Greeley R., Grotzinger J., Haskin L., Herkenhoff K. E., Hviid S., Johnson J., Klingelhofer G., Knoll A., Landis G., Lemmon M., Li R., Madsen M. B., Malin M. C., McLennan S. M., McSween H. Y., Ming D. W., Moersch J., Morris R. V., Parker T., Rice J. W. Jr., Richter L., Rieder R., Sims M., Smith M., Smith P., Soderblom L. A., Sullivan R., Wänke H., Wdowiak T., Wolff M., and Yen A. 2004a. The Spirit Rover's Athena science investigation at Gusev crater, Mars. *Science* 305:794–799.

Squyres S. W., Arvidson R. E., Bell J. F. III, Bruckner J., Cabrol N. A., Calvin W., Carr M. H., Christensen P. R., Clark B. C., Crumpler L., Marais D. J. D., d'Uston C., Economou T., Farmer J., Farrand W., Folkner W., Golombek M., Gorevan S., Grant J. A., Greeley R., Grotzinger J., Haskin L., Herkenhoff K. E., Hviid S., Johnson J., Klingelhofer G., Knoll A. H., Landis G., Lemmon M., Li R., Madsen M. B., Malin M. C., McLennan S. M., McSween H. Y., Ming D. W., Moersch J., Morris R. V., Parker T., Rice J. W., Jr., Richter L., Rieder R., Sims M., Smith M., Smith P., Soderblom L. A., Sullivan R., Wänke H., Wdowiak T., Wolff M., and Yen A. 2004b. The Opportunity Rover's Athena science investigation at Meridiani Planum, Mars. *Science* 306:1698–1703.

Squyres S. W., Arvidson R. E., Blaney D. L., Clark B. C., Crumpler L., Farrand W. H., Gorevan S., Herkenhoff K. E., Hurowitz J., Kusack A., McSween H. Y., Ming D. W., Morris R. V., Ruff S. W., Wang A., and Yen A. 2006.

Rocks of the Columbia Hills. *Journal of Geophysical Research* 111:E02S11. doi:10.1029/2005je002562.

Squyres S. W., Aharonson O., Clark B. C., Cohen B. A., Crumpler L. S., de Souza P. A., Farrand W., Gellert R., Grant J., Grotzinger G., Haldemann A., Johnson J. R., Klingelhoefer G., Lewis J. S., Li R., McCoy T. J., McEwen A., McSween H. Y., Ming D., Moore J. M., Morris R. V., Parker T. J., Rice J. W., Ruff S. W., Schmidt M. E., Schroder C., Soderblom L., and Yen A. 2007. Pyroclastic activity at Home Plate in Gusev Crater, Mars. *Science* 316:738–742.

Squyres S. W., Arvidson R. E., Ruff S., Gellert R., Morris R. V., Ming D. W., Crumpler L., Farmer J. D., Des Marais D. J., Yen A., McLennan S. M., Calvin W., Bell J. F. II, Clark B. C., Wang A., McCoy T. J., Scmidt M. E., and de Souza Jr., P. A. 2008. Detection of silica-rich deposits on Mars. *Science* 320:1063–1067.

Squyres S. W., Arvidson R. E., Bell J. F. III, Calef F. III, Clark B. C., Cohen B. A., Crumpler L., de Souza P. A., Jr., Farrand W., Gellert R., Grant J., Herkenhoff K. E., Hurowitz J., Johnson J., Jolliff B. L., Knowll H., McLennan S. M., Ming D., Mittlehfehldt D. W., Parker T. J., Paulsen G., Rice M. S., Ruff S. W., Schöder C., Yen A. S., and Zacny K. 2012. Ancient impact and aqueous processes at Endeavour crater, Mars. *Science* 336:570–576.

Stanley B. D., Hirschmann M. M., and Withers A. C. 2011. CO_2 solubility in Martian basalts and Martian atmospheric evolution. *Geochimica et Cosmochimica Acta* 75:5987–6003. doi:10.1016/j.gca.2011.07.027.

Stanley B. D., Schaub D. R., and Hirschmann M. M. 2012. CO_2 solubility in primitive Martian basalts similar to Yamato 980459, the effect of composition on CO_2 solubility of basalts, and the evolution of the Martian atmosphere. *American Mineralogist* 97:1841–1848. doi:10.2138/am.2012.4141.

Swindle T. D., Treiman A. H., Lindstrom D. J., Burkland M. K., Cohen B. A., Grier J. A., Li B., and Olson E. K. 2000. Noble gases in iddingsite from the Lafayette meteorite: Evidence for liquid water on Mars in the last few hundred million years. *Meteoritics & Planetary Science* 35:107–115.

Tosca N. J., McLennan S. M., Dyar M. D., Sklute E. C., and Michel F. M. 2008. Fe oxidation processes at Meridiani Planum and implications for secondary Fe mineralogy on Mars. *Journal of Geophysical Research* 113:E05005. doi:10.1029/2007JE003019.

Treiman A. H. 1998. The history of Allan Hills 84001 revised: Multiple shock events. *Meteoritics* 33:753–764.

Treiman A. H. 2005. The nakhlite meteorites: Augite-rich igneous rocks from Mars. *Chemie der Erde* 65:203–270.

Treiman A. H., Barrett R., and Gooding J. 1993. Preterrestrial aqueous alteration of the Lafayette (SNC) meteorite. *Meteoritics* 28:86–97.

Treiman A. H., Gleason J. D., and Bogard D. D. 2000. The SNC meteorites are from Mars. *Planetary and Space Science* 48:1213–1230.

Wallace P. J. 2003. From mantle to atmosphere: Magma degassing, explosive eruptions, and volcanic volatile budgets. In *Developments in volcanology*, edited by de Benedetto V. and Robert J. B. Amsterdam: Elsevier. pp. 105–127.

Wallendahl A., and Treiman A. H. 1999. Geochemical models of low-temperature alteration of Martian rocks (abstract

#1268). 30th Lunar and Planetary Science Conference. CD-ROM.

Wang A., Bell J. F. III, Li R., Johnson J. R., Farrand W. H., Cloutis E. A., Arvidson R. E., Crumpler L., Squyres S. W., McLennan S. M., Herkenhoff K. E., Ruff S. W., Knudson A. T., Chen W., and Greenberger R. 2008. Light-toned salty soils and coexisting Si-rich species discovered by the Mars exploration rover spirit in Columbia Hills. *Journal of Geophysical Research*. 113: E12S40.

Webster J. D. 1990. Partitioning of F between H_2O and CO_2 fluids and topaz rhyolite melt. *Contributions to Mineralogy and Petrology* 104:424–438.

Webster J. 1997. Chloride solubility in felsic melts and the role of chloride in magmatic degassing. *Journal of Petrology* 38:1793–1807.

Webster J. D., Kinzler R. J., and Mathez E. A. 1999. Chloride and water solubility in basalt and andesite melts and implications for magmatic degassing. *Geochimica et Cosmochimica Acta* 63:729–738.

Williams R. M. E., Grotzinger J. P., Dietrich W. E., Gupta S., Sumner D. Y., Mangold N., Malin M. C., Forni O., Ollila A., Newsom H., Dromart G., Palucis M. C., Yingst R. A., Anderson R., Herkenhoff K., Le Mouelic S., Stack K., Madsen M., Koefoed A., Jensen J. K., Goetz W., Bridges J. C., Schwenzer S. P., Rubin D., Pariser O., Deen R. G., and the MSL Science Team. 2013. Martian fluvial conglomerates at Gale crater. *Science* 340:1068–1072.

Wilson L. 1980. Relationships between pressure, volatile content and ejecta velocity in three types of volcanic explosion. *Journal of Volcanology and Geothermal Research* 8:297–313.

Wilson L. and Head J. W. 2007. Explosive volcanic eruptions on Mars: Tephra and accretionary lapilli formation, dispersal and recognition in the geologic record. *Journal of Volcanology and Geothermal Research* 163:83–97.

Yen A. S., Mittlefehldt D. W., McLennan S. M., Gellert R., Bell J. F., McSween H. Y., Ming D. W., McCoy T. J., Morris R. V., and Golombek M. 2006. Nickel on Mars: Constraints on meteoritic material at the surface. *Journal of Geophysical Research* 111:E12S11. doi:10.1029/2006JE002797.

Yen A. S., Morris R. V., Clark B. C., Gellert R., Knudson A. T., Squyres S., Mittlefehldt D. W., Ming D. W., Arvidson R., McCoy T., Schmidt M., Hurowitz J., Li R., and Johnson J. R. 2008. Hydrothermal processes at Gusev crater: An evaluation of Paso Robles class soils. *Journal of Geophysical Research: Planets* 113:S06S10. doi:10.1029/2007je002978.

Yingst R. A., Crumpler L., Farrand W. H., Li R., and de Souza P. 2010. Constraints on the geologic history of "Home Plate" materials provided by clast morphology and texture. *Journal of Geophysical Research* 115:E00F13. doi:10.1029/2010JE003668.

Zolotov M. Y. and Mironenko M. V. 2007. Timing of acid weathering on Mars: A kinetic-thermodynamic assessment. *Journal of Geophysical Research* 112:E07006.

Zolotov M. Y. and Shock E. L. 1999. Abiotic synthesis of polycyclic aromatic hydrocarbons on Mars. *Journal of Geophysical Research* 104:14033–14049.

APPENDIX

FORMATION PROCESSES OF ALTERATION PHASES COMPARISON WITH MARTIAN METEORITES

We discuss a brief excursion to alteration within two classes of Martian meteorites. This allows us to understand the alteration assemblages, which are not observable from orbit, but are found in the Martian meteorites, and the conclusions deducible from these observations.

The Martian meteorite ALH 84001 could provide an analog for the observations in the Gusev crater. It has been suggested to stem from the basement of a large crater (Treiman 1998) and contains carbonates (e.g., Harvey and McSween 1996; Gleason et al. 1997; Kring et al. 1998; Treiman 1998), for which a wide range of formation temperatures from ambient to exceeding 650 °C have been suggested (e.g., Kirschvink et al. 1997). In contrast to ALH 84001, in which only carbonates have been found so far, the nakhlite Martian meteorites contain a wider variety of alteration phases (Treiman et al. 1993; Bridges and Grady 2000; Treiman 2005; Changela and Bridges 2010). The alteration mineralogy in the nakhlite meteorite Lafayette consists of an early ankeritic carbonate stage, followed by phyllosilicates and a late gel formation (Changela and Bridges 2010), with the phyllosilicate being dominantly saponite and the gel being ferric (Hicks et al. 2012). The Lafayette alteration has been dated to be 670 Ma old only (maximum age; Swindle et al. 2000), thus formed while Mars' surface was cold and dry. Recently, it has been suggested that the heat source for nakhlite alteration was an impact into the nakhlite pile (Changela and Bridges 2010; Bridges and Schwenzer 2012), which was confirmed by dissolution following the olivine [001] in Nakhla (Lee et al. 2013). The ankerite formation in the presence of dissolving Lafayette requires a fluid temperature of >150 °C, while the phyllosilicates form at significantly lower temperature (approximately 50 °C) (Bridges and Schwenzer 2012). Helium data indicate more significant loss than what the low shock pressure of the nakhlites suggests (Schwenzer et al. 2008), which could indicate that they experienced two shock events (one causing the hydrothermal overprint, the second launch from Mars) and the loss due to heating from the hydrothermal activity (Bridges and Schwenzer 2012).

Magmatic hydrothermal alteration has also been suggested for the alteration mineralogy seen in the

nakhlite Miller Range (MIL) 03346 (McCubbin et al. 2009). Pyroxene-hosted melt-inclusions contain jarosite and hematite in addition to titanomagnetite, pyrrhotite, potassic-chlorohastingsite, an iron-rich silicate glass, and possibly goethite. On the basis of textural and chemical analyses of the melt inclusion mineralogy, McCubbin et al. (2009) concluded that the jarosite, hematite, and possibly goethite within the melt inclusions formed under hydrothermal conditions from a chlorine-rich magmatic fluid. Jarosite has also been found interstitially in some nakhlites found in Antarctica, but, based on textural analyses, these sulfates are thought to be terrestrial alteration and not Martian jarosite (e.g., Noguchi et al. 2009; Changela and Bridges 2010; Hallis and Taylor 2011). Filiberto and Treiman (2009) also noted that the magma or fluid that produced the potassic-chlorohastingsite in MIL 03346 was chlorine-rich and the calculated Cl concentration (16 wt% Cl) is in excess of chlorine saturation values for a magma (approximately 3 wt% Cl; Webster et al. 1999), suggesting magmatic hydrothermal conditions. Therefore, the nakhlite Martian meteorites might themselves host two generations of hydrothermal alteration phases, whereby one is preserved in melt-inclusions and the second contained in fractures. We next focus on comparing the fracture-hosted meteoritic alteration assemblage to our model results.

Our models predict phyllosilicate formation at all modeled temperatures and a wide range of W/R, but quantities and assemblages vary significantly. Chlorite and serpentine form at 300 °C and W/R>10000 (Fig. 1). At 150 °C in the CO_2 poor case (Fig. 2), a wider variety is observed: kaolinite forms at high W/R between 10000 and 900. Nontronite forms at lower W/R between 2000 and 400, while chlorite formation sets in at W/R of 900 and continues down to W/R of 1 with a maximum of formation at approximately 10. Small amounts of serpentine form between W/R of 200 and 10 and then around W/R of 1 again. The presence of CO_2 changes the phyllosilicate precipitation significantly, because Ca, Mg, and Fe are bound as carbonates forcing kaolinite formation over a wide W/R range. Only after the concentration of those cations exceeds the amount bound in carbonate will chlorite form. This is different at 13 °C, where carbon dioxide has a much higher solubility and thus carbonate formation sets in at W/R of approximately 500 only (Fig. 2). Nontronite is therefore precipitated at higher W/R, and chlorite occurs throughout the entire W/R range, similar to the CO_2-poor case.

Compared with observations in the meteorites, ALH 84001-type alteration with pure carbonate formation calls for high CO_2-concentration in the fluid or even vapor phase or a multistage alteration with separation of the ions not needed for carbonate precipitation (e.g., Al, Si) before carbonate formation. All options have been considered before from petrologic and modeling studies (e.g., Griffith and Shock 1995; Gleason et al. 1997; Schwenzer and Kring 2009c). Nakhlite type alteration as observed in Lafayette (Changela and Bridges 2010) reveals a drop in CO_2-concentration and temperature (Bridges and Schwenzer 2012). This brief excursion to the Martian meteorites demonstrates that, to understand the formation conditions of the Columbia Hills alteration minerals and silica deposits, the alteration assemblage matters.